Cornwall FLOW Accelerator

WP4 INNOVATION IN LOW CARBON DESIGN AND MANUFACTURABILITY – Report 2: Manufacturing Variants and Future Steps

Document Title		WP4 INNOVATION IN LOW CARBON DESIGN AND MANUFACTURABILITY – Report 2: Manufacturing Variants and Future Steps	
Document Reference		PN000463 CFAR-OC-043-14032023	
Date of Issue		14/03/2023	
Authors		Oliver Nixon Pearson, Peter Greaves, Dimitrios Mamalis, Konstantinos Bacharoudis	
Revision History	**Date**	**Reviewed / Approved by**	**Authorised by**
First Draft	01/12/2022 (V1)	Mark Forrest	
Second Draft			
First Issue	07/03/2023 (V2)	Mark Forrest	Simon Cheeseman

HM Government

European Union
European Regional Development Fund

CORNWALL EDRF PRIORITY AXIS 4 LOW CARBON FOW

WP4 INNOVATION IN LOW CARBON DESIGN AND MANUFACTURABILITY – Report 2: Manufacturing Variants and Future Steps.

GENERIC REPORT

Authors: Oliver Nixon Pearson, Peter Greaves, Dimitrios Mamalis, Konstantinos Bacharoudis.

Date: 01/12/2022

In partnership with:

DOCUMENT HISTORY

Revision	Date	Prepared by	Checked by	Approved by	Revision history
1	01/12/2022	Oliver Nixon Pearson, Peter Greaves, Dimitrios Mamalis, Konstantinos Bacharoudis	Mark Forrest	Simon Cheeseman	1
2	7/3/2023		Mark Forrest		

TABLE OF CONTENTS

LIST OF FIGURES

LIST OF TABLES

ABBREVIATIONS

AEP	Annualised Energy Production
ALM	Additive Layer Manufacture
AM	Additive Manufacture
ATOM	Aeroelastic Turbine Optimisation Methods
BIAX	Biaxial (Fibre architecture)
CAPEX	Capital Expense
CT	Cycle Time
DC	Double Cut
DLC	Design Load Cases
DV	Design Variable
EUR	Euro (Currency)
FEP	Fluorinated ethylene propylene
GCMMA	Globally Convergent Method of Moving Asymptotes
GWP	Global Warming Potential
HAWT	Horizontal Axis Wind Turbine
IEA	International Energy Agency
IEC	International Electrotechnical Commission
LCoE	Levelized Cost of Energy
LCA	Life Cycle Analysis
LDT	Levenmouth Demonstration Turbine
LE	Leading Edge
MDO	Multi-disciplinary optimisation
MW	Megawatt
NCC	National Composites Centre
NREL	National Renewable Energy Laboratory
OEM	Original Equipment Manufacturer
OPEX	Operational Expense
ORE	Offshore Renewable Energy Catapult
PET	Polyethylene terephthalate
PVC	Polyvinyl Chloride
RTM	Resin Transfer Moulding
RTV	Room Temperature Vulcanized
RVB	Reusable vacuum bag
SAN	Styrene acrylonitrile resin
SNL	Sandia National Laboratory
TE	Trailing Edge
UD	Unidirectional
UK	United Kingdom
US	United States
VARTM	Vacuum Assisted Resin Transfer Moulding
WBRH	Wind Blade Research Hub
WISDEM	Wind-Plant Integrated System Design and Engineering Model

1 Introduction

1.1 Project overview and Aims

The Cornwall FLOW Accelerator project (CFA) aims to develop, accelerate, and spearhead the industrialisation of floating offshore wind in the Celtic Sea. It will accelerate the region's readiness for large scale Floating Offshore Wind (FLOW) and will fast-track development of the region's capacity to build-out large-scale wind farms in the Celtic Sea from 2025 onwards. This puts the Celtic Sea in a position to make a significant contribution to the UK's offshore wind energy targets through development of a new floating wind industry that can create thousands of jobs with huge export potential. Also, this will generate many more R&D opportunities in the area. Floating platforms can access stronger winds in deeper waters than conventional fixed land-based turbines. The Celtic Sea has some of the most prominent wind resources in Europe. By 2025, the region will be prepared for the first 500 MW FLOW farms. The ambition for FLOW in the Celtic Sea will deploy 4GW by 2035 and a further 20GW by 2045. The South-West region has world-leading floating wind research expertise and academic test facilities. The project will utilise these for new product and service development for industrial partners, building clear routes to market as well as de-risking initial investment. The focus of this report aims to define the current state-of-the-art in offshore Horizontal Axis Wind Turbine (HAWT) blade manufacture, and to determine the best opportunities for low-carbon and environmentally friendly cost-effective processes for potential port development for blade production. Also, future blade concepts will be explored to determine feasibility.

The main scope of this report is for production of the next generation of turbine blades with reduced environmental impact, and with the next generation of recyclable materials in the manufacturing process. Part 1 of this report contained a desk-based benchmarking study into the opportunities for low carbon manufacture of turbine blades, which outlines the current state-of-the-art and explores some concepts for the immediate future of blade manufacturing in the Southwest. It explored the current state-of-the-art in terms of cost modelling for a standard reference blade (15MW) and suggests short term improvements. The report also provided a reference case for the Life Cycle Analysis (LCA) along with a literature review on recyclability and sets the scene by introducing the different manufacturing variants which will be the focus of this report. This is the second of a two-part report which sets out to highlight future opportunities in blade manufacturing and to identify areas of potential cost saving, and to elaborate on the different manufacturing scenarios to determine any potential cost benefit.

2 Major Cost Drivers

2.1 Overview of the Current Blade Moulding Process

A review of the current blade manufacturing process is given in report #1 titled 'Wind Turbine Blades Design and Manufacturing, Current State-of-the-Art Literature Review', and so a short section here will summarise the current blade moulding process for completeness. The major step change to improving

the blade moulding process came about with the introduction of vacuum technology, which includes vacuum infusion of dry preforms and pre-impregnated fibre tapes, denoted as prepregs. These are tapes of fibres which have already been pre-impregnated with resin by the manufacturer and are typically laid up in stacks prior to autoclave curing. Vacuum infusion is the most widely used technology to produce large wind blades to date, due to its ease of scalability. In vacuum infusion processes, dry fibres are placed into closed moulds and sealed using tacky tapes as a sealant around a disposable bagging material, where resin is injected into the cavity or bag under pressure. After the resin has filled the areas between the fibres, the component is then cured. The blades are among the most critical structures of the turbine given that catastrophic failure of a blade can lead to knock-on failure of other turbine components.

The primary function of a wind turbine blade is to capture the wind and transfer the load to the shaft, which creates a bending moment on the root bearing, and a torque on the main shaft. A blade is effectively a large cantilever beam, loaded primarily in two ways. Flapwise, or out-of-plane, bending loads arise from aerodynamic forces and edgewise, or in-plane/bending which arises from the blade self-weight.

The blade structure is designed to withstand these loads whilst having a form which is as close as possible to the optimal aerodynamic shape. The suction side and pressure side shells are large aerodynamic panels designed to “catch the wind” and transfer the loads to the spar caps. They are comprised of a lightweight core material sandwiched between triaxial glass fibre fabric (as can be seen in Figure 1).

They are typically moulded in two “blade shell” tools, and adhesively bonded to each other along their leading and trailing edge, and to the spar caps in the middle. Shell skins are lightweight triaxial glass fibre skins, of low thickness; they therefore need to be stabilised using a lightweight core (typically made from balsa wood or PVC foam) to prevent buckling. The shells are bonded together at the leading and trailing edges. The infusion process typically involves the use of large amounts of consumables which are discarded after each infusion operation, which adds considerable costs to the overall manufacturing waste stream, this is a topic which will be discussed in the next section.

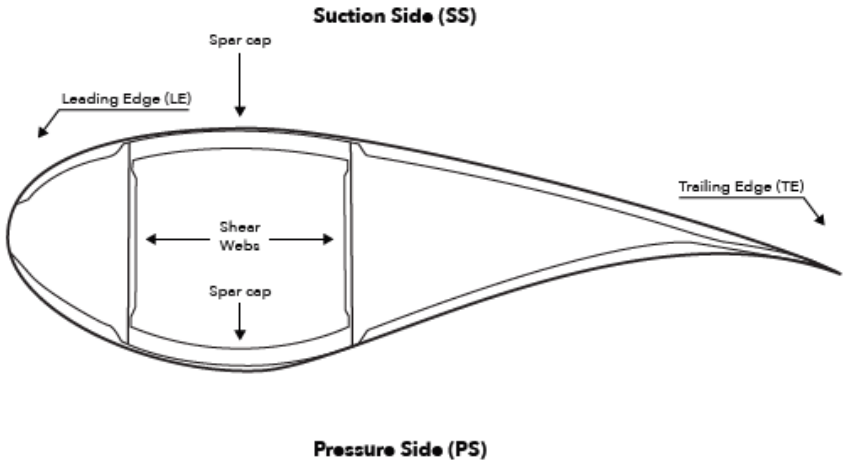

Figure 1. Wind Blade Cross Section Terminology

The spar caps are generally made of uniaxial material (often carbon fibre instead of glass for modern

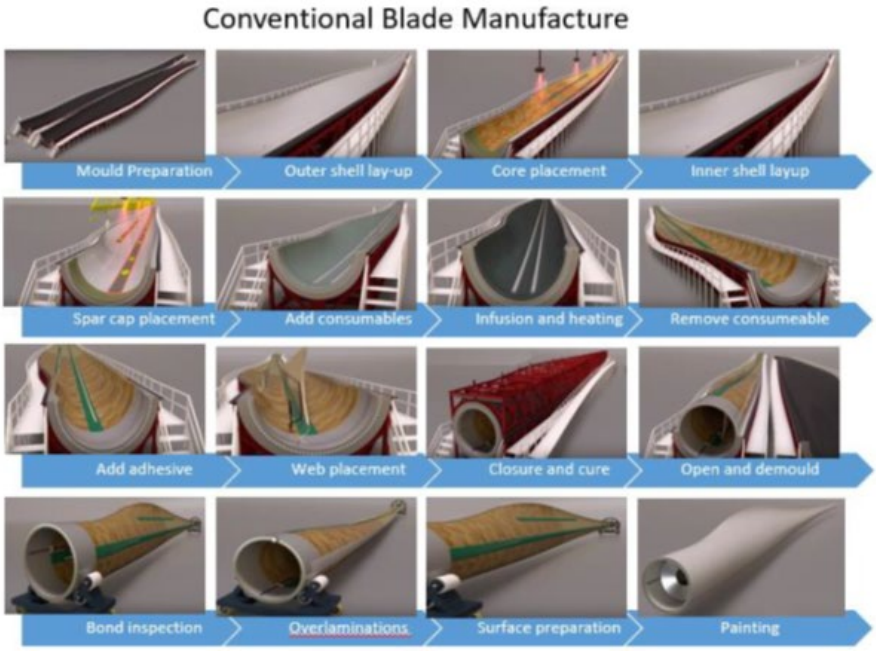

offshore blades) placed at the thickest part of the section to maximise their contribution to the bending stiffness. The shear webs transfer the forces between the spar caps and are typically made of biaxial glass fabric with a core material (again made from balsa wood or PVC foam). Figure 2 shows a schematic of the conventional blade manufacturing process.

Figure 2. Conventional Blade Manufacturing Process

2.2 Waste Stream

Waste arises not only at the end-of-life (EoL) of a turbine blade, but also through the entire blade lifecycle including the manufacturing process, transportation, maintenance, and operation. The manufacturing in-process waste can be estimated by subtracting the total finished blade mass from the bill of materials. The Bill of Materials (BoM) contains the quantities and types of the raw materials used during the manufacturing process including fibre fabric, resin, structural adhesives, core, paint, metal accessories and manufacturing process consumable materials. It does not include working protection consumables such as gloves, masks, containers, or packaging. Analysis of 21 BoMs provided by three blade manufacturers for blades manufactured from glass fibre and epoxy resin using VARTM technology revealed that the in-process waste was between 12-30%, with a median value of 17%, of the finished blade mass (Liu 2015). Manufacturing waste is the waste generated throughout manufacturing stage and consists mainly of dry fibre offcuts, composite offcuts, resin residue and vacuum consumables. It is therefore to be determined, whether the use of reusable systems for the infusion process could be adopted to reduce the extent of the waste stream.

2.2.1 Introduction to Reusable Bagging Materials

Durable elastomeric custom produced bags could cut consumables and increase production rate. Manufacturers are always looking for opportunities to reduce costs where an increasing number of infusion suppliers are finding solutions to this.

Typically, the weights are around 8-10 kg per square meter and so at scale any reusable vacuum bag technology would need expensive lifting and handling equipment, along with careful consideration in storage method and storage space to optimise their lifespan.

A growing number of manufacturers as well as some of those in aerospace are beginning to find these advantages in reusable vacuum bag (RVB) technology. Proponents indicate that silicone elastomeric bags may be able to replace disposable bagging films. Advantages include improved part-to-part quality and greater shop safety and cleanliness. Likewise, they provide a way to cut down on consumables such as tacky tapes and reduce a shop's waste stream. However, RVBs will require additional capital expenditure and offer challenges that must be overcome prior to implementation, and they aren't always advantageous in every part process situation.

Each RVB system have their advantages and disadvantages, which fabricators would need to consider e.g., the relative ease of building and using the RVB, its tolerance for a specific resin chemistry and processing temperature, and, most importantly, the aggregate cost per square foot.

RVBs can be produced using synthetic or natural rubbers. The most common synthetics, include a broad range of silicones, however other elastomeric materials have been used in vacuum membranes, for example forms of polyurethane, ethylene/propylene, polysulfide, fluorosilicone, nitrile and chloroprene.

Silicones are polymerised siloxanes, or polysiloxane, an inorganic/organic polymer. Thus, they consist of an inorganic silicon/oxygen backbone where organic groups (methyl, ethyl or phenyl), derived from petroleum distillates, are used. Formulated to exhibit rubber-like elongation, silicone rubber is a common RVB material. To be useful as RVB materials, silicones require in-situ polymerization via the addition of a catalyst which is typically platinum, but also tin, where their cure can vary with environmental conditions.

Silicone sheet materials, especially high-strength compounds that are postcured for higher heat resistance, have been used for decades as membranes, diaphragms, and envelope bags in production tooling. Major suppliers of silicone sheet goods and liquid formulations include Wacker Chemical Corporation (Munich, Germany), Arlon Silicone Technologies (Bear, Del.), Dow Corning Corp. (Midland, Mich.), Shin Etsu Silicones of America (Tokyo, Japan), Mosites Rubber Co. (Ft. Worth, Texas) and ACC Silicones Europe (Amber House, Bridgwater, Somerset, U.K.).

Silicone bagging materials have moved from high-end autoclave applications to low-cost infusion applications, after suppliers began offering room-temperature vulcanizing (RTV), lower-viscosity, two-part, platinum-cured silicone formulations. These forms were stable, more user-friendly, have good

properties and can be sprayed, poured, or brushed into position to create a custom silicone bag for infusion.

Various approaches can be used to fabricate a custom RVB for low-temperature, out-of-autoclave cures, including seaming silicone sheet stock, however the fastest and most common method is to use a dedicated spray machine that employs either an atomizing spray head or a splatter-type head which generates a film directly on the mould. Multiple layers are built up to the desired RVB thickness, typically from around 1 mm to 10 mm. The working pot times, air assist velocity needed for spraying, spray equipment clean-up requirements and specifics like final bag thickness vs. weight and cure time vary by material type and supplier. Many different types of edge seal are available, and many are proprietary or based on patent-pending technology. The simplest seal for a frameless RVB is a half-round or V-shaped profile affixed to the lower tool's flat flange, which is then covered with the elastomer spray. After cure, the profile is pulled out, leaving a channel a few inches from the RVB edge.

Vacuum and resin ports are created by bonding port components to the bag or placing them at various desired locations, masking them against the spray and then spraying the silicone material over them. Resin flow channels can also be designed into the bag itself. When a vacuum is pulled through the ports and the perimeter channel, the RVB is pulled against the tool. However, there are also other methods of vacuum sealing.

Both silicone and natural rubber offer benefits for certain applications and have process and handling similarities, together with some uniquely individual characteristics. An important similarity is that epoxy resins will attack all types of RVBs, breaking them down at a faster rate than polyester or vinyl ester resins. It has been said that the silicone chemistry is formulated for tear strength and is an important criterion when selecting a bagging system and it can directly correlate to bag life. In terms of heat resistance, natural and silicone rubbers differ. There are autoclave-suitable silicone RVBs that can take temperatures as high as 240°C. Natural rubbers normally can't tolerate such high temperatures.

On the issue of weight, RVBs get heavy when they are fabricated for larger parts. Each supplier's material will vary in terms of coverage per pound of liquid, however an RVB for a 3m x 3m part can approximately weigh 30 kg or more, which is greater than one person could comfortably handle therefore logistics become more important. Designing edge frames and lifting points will become a requirement with oversize systems. This will in turn add further weight, and the requirement for heavier lifting equipment will result in greater CAPEX.

If silicones aren't properly processed, they can transfer material from the bag to parts, however that is less of an issue if the part isn't being finished or painted on the part surface. The use of barrier films, such as fluorinated ethylene propylene (FEP) release films, can prevent transfer from the bag to the surface. Also, silicone and natural-rubber membranes can be easily repaired when torn for example using overlaid doubler patch.

2.2.1.1 Sprayable Silicone Bags

Prairie Technology Group were the first organisation to patent a spray-on RVB in 2006 (U.S. Patent number 7014809B2). The concept involves a technique of creating a reusable flexible polymer bag or skin which utilises a spray (or swirl spray) application of a sprayable polymer, where the bag or skin is used as a bagging material to be used in the resin transfer moulding process (infusion or vacuum bagging process) for fabrication of glass or carbon fibre reinforced plastic parts.

A benefit of this technique is a viscosity low enough that the silicone can be atomized, instead of splattered, along with the propensity to adhere to itself upon application of successive layers either when previous layers have cured or uncured. Some vendors also rent out the equipment with operator training and could reduce CAPEX for short numbers of runs. Many edge seal designs can be offered.

Bags with thickness variations can be produced where the thick sections can act as pressure intensifiers for key regions of the part. Fabrics can be added for further reinforcement; however, it isn't a requirement, but it can help support placement of the vacuum channel and ports. Another recommendation for larger bag sizes, is to add hard anchor points along the bag margins, integrated with cloth reinforcement so that the RVB can be safely and easily lifted with an overhead crane or lifting system.

2.2.1.2 Silicone RVB's physical and technical properties

These are the main technical factors to be considered in the silicones to be used in Reusable Vacuum Bag moulding:

- **Viscosity**

Finding the right balance between the vacuum infusion method used and final product characteristics, including flowability versus non-sag. Thixotropy, which is the change of the composite resin in viscosity from the beginning to the end of the process, must also be factored in.

- **Chemical resistance**

This is without any doubt the most important property of the specific bag to be used in each process and the one that will determine whether silicone RVBs are the right choice versus other techniques. Bag wear is caused by chemical reactions between the resin and the silicone. The key is to determine the improvement in resistance to other chemicals, by reducing or lowering the time the casting material is in contact with the silicone surface and choosing the resin characteristics and mould design. For example, low viscosity and long curing resins penetrate the silicone bag more, as does low heat dissipation.

- **Hardness, elongation, tear, and tensile strength**

This is the main factor that must be measured and calibrated so that the RVBs have the right mechanical properties for the application. The bag must be sufficiently flexible and resistant and have

the right hardness. At times, where more tension resistance or rigidity is required, different textiles can be added in the bag design.

- **Mould size**

For big moulds, resin must flow easily and therefore have low viscosity and long curing time to allow the mould to be filled completely. This is a major complexity to be dealt with to determine if an RVB will resist properly for big moulds. It should be noted that for very large moulds, such as full-sized wind turbine blades, silicone RVBs may not be suitable since the weight of the silicone in an RVB may be too high to process.

- **Number of casts per bag**

Given all the factors that come into play, it is difficult to predict the number of casts that any single mould can ensure. This is first and most important question customers are concerned with and therefore our experts must define if the silicone bag technology we propose is convenient and cost-effective versus other composite manufacturing processes.

- **Curing time and temperature**

Generally, most manufacturers want to accomplish this part of the process in a few minutes and, if possible, at room temperature.

2.2.1.3 The versatility of silicone polymers

Silicones are inert synthetic compounds that come in a variety of forms: oils and gums that can be formulated in fluids (emulsions, resins, greases, compounds) or elastomers (HCR, LSR, RTV-1 or RTV-2). Thanks to their versatility, silicones are used in a wide range of industrial applications. Therefore, silicones products are present/used in many moulding processes, such as prototyping, serial parts manufacturing, tire curing, fabrication of prostheses and medical devices, and the production of precision parts in many industries. Silicones ensure that moulded products are true to the original in every detail and offer mould durability, flexibility, fidelity, and resistance to resins. The other major advantage is that silicones, compared to other materials, such as rubber or certain plastics, are available in various viscosities and can be cured at room temperature. Beyond moulding, all advanced technological devices, from smart phones to electrical vehicles, use silicone for sealing, bonding, potting, and encapsulating and protecting micro-electronics.

2.2.1.4 Traditional composite moulding methods vs RVBs

Composites are traditionally moulded by pouring the resins and fibres into disposable plastic bagging sheets that are manually placed and assembled by highly skilled operators. Various techniques are used, including vacuum infusion, RTM, RTM light and manual lamination. These techniques all generate high labour costs and time-consuming preparation and processing, which means that assembling the mould may take several hours, and even several days in some cases. This method also generates a great deal of waste since every mould requires a change of plastic bagging and therefore

is not environmentally friendly, also adding cost since the plastic waste is contaminated with resins that cannot be included in common disposal systems.

In recent years, manufacturers have begun to use Silicone-based Reusable Vacuum Bag (RVB) membranes that increase productivity, reduce costs (for high-volume serial production) and improve the quality and consistency of parts produced. This process also contributes to better industrial safety and workplace cleanliness, while reducing the use of consumables and thus lowering waste.

A comparison of the traditional composite moulding methods including advantages, drawbacks, and applicability of each of these methods to different products and processes is presented in Table 1. This will then serve as a base to determine where Vacuum Infusion Moulding using RVBs could become a viable alternative for you. Furthermore, figure 3 presents the cumulative costs against the number of parts are manufactured for classic resin infusion process against reusable vacuum infusion with silicone bags.

Table 1 Traditional composite moulding methods i.e., advantages, drawbacks, and applicability.

Type of molding process	Initial investment	Sat-up cost	Operator safety	Cost of machinery	Technical knowledge required	Manufacturing time	Waste material generated	Final quality and versatility	Serial production efficiency	Total cost of ownership
Manual lamination	Low	Low	Low	None	Low	Long	High	Low	Low	Low for small batches
Resin Transfer molding (RTM)	High	Medium	Medium	High	High	Short	Medium	High	Medium	Medium
RTM Light	High	Medium	Medium	High	High	Short	Low	High	Medium	Medium
Reusable Vacuum Bags (RVBs) A&B	High	Low	High	Medium	Medium	Short	Low	High	High	Low for large series

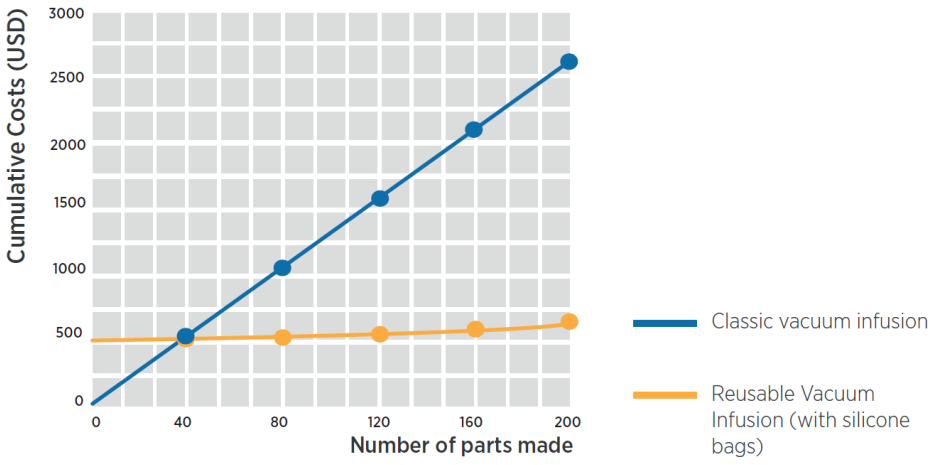

Figure 3 Cumulative costs against the number of parts are manufactured for classic resin infusion process against reusable vacuum infusion with silicone bags. Note that the price of a RVB is ~70$ per square meter [18].

2.2.1.5 The underlying chemistry of silicone polymers

This versatility is based on the fact that silicones are polymers containing silicon, combined with carbon, hydrogen and oxygen and, in some cases, other elements to achieve specific process and performance features. The basic structure of silicones:

Silicones are made up of polyorganosiloxanes, where silicon atoms are linked to oxygen to create the siloxane bond. The remaining valences of silicon are linked to organic groups, mainly methyl (CH3):

• Polydimethylsiloxane (FLD 47)

• Phenyl, vinyl, hydrogen

Key properties of silicones

• Room temperature curing

• High-performance release properties, particularly useful in moulding

• Thermal stability (from -80°C to 250°C), ensuring proper viscosity in a wide temperature range, which means good upstream process uniformity (excellent spread and coating capabilities) and reliable downstream operating performance in extreme weather conditions

• Resistance to natural ageing (oxidation, UV)

• Low hardness

• Low modulus for compensation of stress in high temperature or cycling conditions.

• High fire resistance capabilities, including low emission of smoke and toxic fumes, self-protection,

• Low surface energy; good wetting on many substrates

• Hydrophobia (beading effect) to ensure waterproofing

• Easy re-workability and different adhesion features, depending on requirements

• Extremely low inner stress on potted components, preventing delamination from the housing substrate

2.2.1.6 Current RV tooling market status

Table 2 Market Survey of Commercially available silicone bagging materials suppliers.

Company name	Region	RVB product type/application	Price per m^2 or £/kg
Wacker Chemical Corporation	Munich, Germany	Silicone rubbers (Room temperature curing)	25 Eur/kg small volumes, 22 EUR/kg large volumes
Arlon Silicone Technologies	Bear, Del.	Silicone elastomers	n/a
Dow Corning Corp.	Michigan, US	Silicone liquid formulations	n/a
Vacform Composites	West Yorkshire, UK	Silicone rubbers	£80-100/sqm
Mosites Rubber Co./Aeroconsultants Ltd.	Texas, US	Silicone rubber blankets	200$/sqm
ACC Silicones Ltd.	Somerset, U.K.	Silicone spraying system	n/a
Elkem Silicones	Oslo, Norway	Silicone rubbers	200 – 300 $/sqm
Industrial Technologies	Ohio, US	Cast silicone RVB	n/a
Composite-integration	UK	Silicone spraying system	n/a
Simtech	Belgium	Self-heating reusable vacuum rubber or silicone bags	n/a
Smooth-On, Inc	Pennsylvania, US	Brush-able platinum silicone rubber and spraying system	Not available for larger components
Torr Technologies Inc.	Washington, US	Elastomeric Vacuum Tools; plates, diaphragm, envelopes, heating tables etc.	Not available for larger components

2.2.1.7 General classes of reusable bags

Most common is the use of frame bag for easy and fast open and close in vacuum- and heating tables. A usually flat membrane is mounted in a fixed alignment. In transition of this principle, mobile frame bags with sealing profiles and custom shaped bags can be placed on flanges of existing tools.

b) The principle of frameless flexible bags with integrated sealing solution allows a very easy application (as can be seen in Figure 4):

1. Position the composite part or lay-up in your tool

2. Place the membrane, pay attention to position markers if existing

3. Close the seal by pressing all around so it locks easily

4. Apply vacuum

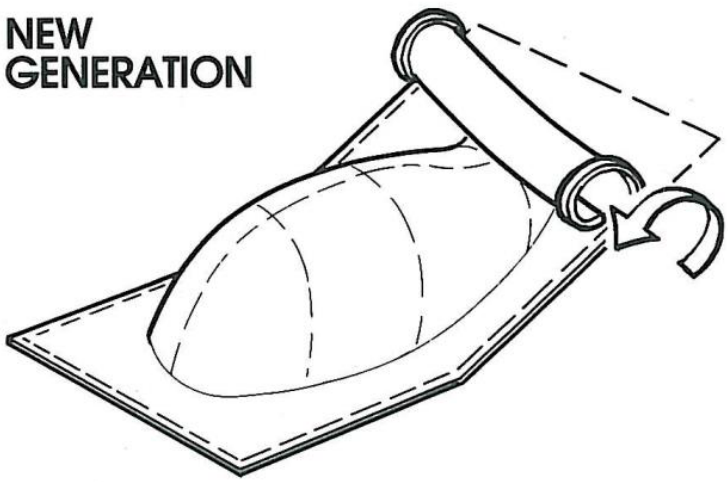

Figure 4 Principle of frameless RVB.

Note that this type of bag, as can be seen in Figure 5, does not require spacious storage and because of the high elongation and robust material, a wrinkle-free conformity to the tool or part shape is given.

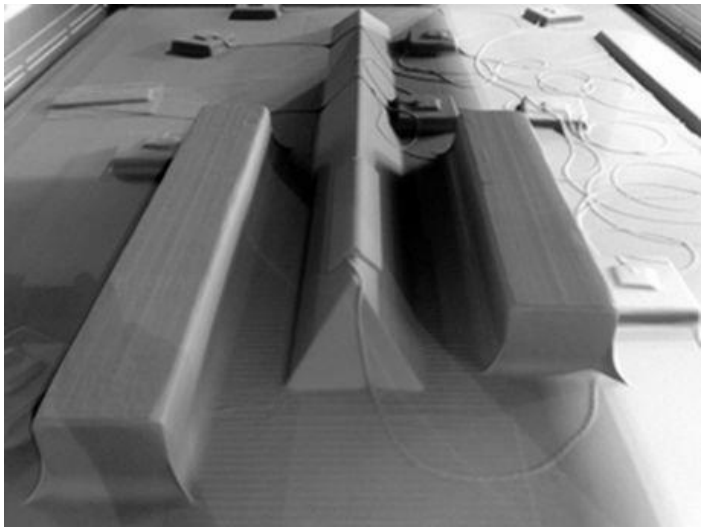

Figure 5 Adaptation of the membrane to the component geometry.

3 Introducing the Variants/Scenarios for Cost Optimisation

3.1 An Introduction to the NREL Cost Model

A technical report describing a detailed blade cost model for wind turbines in the range of 30-100m was developed by the National Renewable Energy Laboratory, a federally funded research and development facility sponsored by the department of energy in the US. The model applies to multimegawatt wind turbine blades manufactured using vacuum-assisted resin transfer moulding, which is the most widely adopted manufacturing method for modern wind turbine blades. The model is implemented both in a large Excel file and in Python. The latter is freely available in the repository of the Wind-Plant Integrated System Design and Engineering Model (WISDEM). WISDEM is a multidisciplinary analysis and optimization design framework developed at the National Renewable Energy Laboratory. This parametric blade cost model represents a valuable research tool to run design optimization studies for wind turbine blades and estimates both fixed and variable costs per blade for a given number of blades produced per year, cycle time, workforce, and other key metrics. Variable costs consist of the costs for the materials, the labour, and the utilities. The fixed costs capture the equipment, tooling, building, maintenance, overhead, and capital. To estimate all these quantities, the number of labour hours and the cycle time (CT) required by the various manufacturing processes are carefully estimated. The fixed and variable costs are then used to construct a parametric virtual model of a blade manufacturing facility. The model is first presented with its approach and assumptions and then computes the costs of three blades, namely the 33-meter-long Wind Partnership for Advanced Component Technologies (WindPACT) study blade, the 63-meter-long International Energy Agency (IEA) Wind Task 37 land-based reference wind turbine blade, and the 100-meter-long SNL-100-03 blade developed at Sandia National Laboratories.

The model is applicable to blades made with a conventional structural-skin geometry, namely two straight spar caps, one or more shear webs, leading- and trailing-edge reinforcements, and an outer shell skin with a sandwich structure. Additionally, the model is valid for blades with mild sweep and prebend. As long as the blade curvature is not excessive, the manufacturing process is unchanged. Finally, the model assumes that spar caps, root inserts, and shear webs are pre-infused and then inserted into the low- and high-pressure skin moulds. The model loses validity for blades characterized by a more complex internal geometry, such as blades with tapered and/or pultruded spar caps, segmented blades, blades made with manufacturing methods different than VARTM, and so on. Blades that deviate from the assumptions of the model require modifications (possibly minor) to the model. The model was initially developed in a blade manufacturing facility to analyse the manufacturing process and identify inefficiencies in labour and cycle times. In a second step of development, the details of the models were developed for cost and manufacturing process modelling. The model involves many assumptions regarding the steps, the work rate for each step, how workers and teams are formed, and so on, and assumes that the key limiting step is the infusion step involving the moulds. These assumptions originate from real blade factories and have been calibrated such that the overall cost and cycle times match available empirical industry data. Originally implemented in a large Excel file, the model has now been implemented in a Python code and coupled to the Wind-Plant Integrated System Design Engineering Model (WISDEM) framework. WISDEM is a multiyear, multidisciplinary design, analysis, and optimization (MDAO) framework developed at the National Renewable Energy Laboratory (NREL) [21] and freely available in an online repository on github.com/WISDEM. MDAO models have been increasingly adopted within the design of wind turbines. These methods offer the opportunity to run design optimization studies in an automatic manner, generating a multitude of results in a relatively limited amount of time. In addition, properly defined automatic design procedures ensure that all synergies and constraints between disciplines are considered at the initial stages of multiple design iterations. This represents undeniable progress compared to former methods, where single discipline experts performed the detailed design of each wind turbine component and only at a second stage integrated all of them together, iterating when necessary. The single iteration design relies on the expertise of the single designers, in which the existing couplings between disciplines can only be captured partially. MDAO aims at providing a valuable alternative. The blade cost model is fully coupled with RotorSE, the rotor design optimization model of WISDEM. This means that each blade cost execution can be called from RotorSE automatically. It is important to highlight that the Python code implementing this model consistently adopts the International System of Units. The Python code implementing the blade cost model works by reading in PreComp input files that describe the outer blade shape and internal structure. PreComp is the standard cross-sectional analysis tool within WISDEM. The PreComp input files are typically generated by Numad, a three-dimensional finite element method pre-processing code implemented in MATLAB and developed at Sandia National Laboratories (SNL).

3.1.1 Limitations of the NREL Cost Model

The model should also be subject of improvements in several areas. To start, the price of foam and balsa wood has so far been assumed proportional to the area, however it is also proportional to the thickness, and that thickness is highly dependent on the location within the blade. The foam core kit

will need further details in terms of the breakdown of costs to include machining of kerfs, design labour costs, and ideally a process flow for the core kit supply and further details pertinent to the contributions to layup. The list of consumables may also be extended, for example, with materials adopted during the finishing operations, as well as the inclusion of bagging materials, infusion mesh, and release films. Additionally, the model should support blade components manufactured via methods alternative to VARTM, such as pultrusion, and Additive Manufacturing, and should be able to estimate the costs of bonded root inserts, which are more and more commonly used, as well as segmented blades. A step of ultrasonic inspection could also be added. This is often performed on the bonding lines and should be part of the labour model as well as the equipment. Similarly, a step for remediation could be added to the labour model. The accuracy of tooling should be improved to include lifting apparatus and jigs and breaking down the tooling costs to include the hinges of the mould which are significant proportion of the mould cost. Further resolution to labour costs could include the time taken for parts of the workforce to migrate around the factory to perform the various tasks required. Finally, the virtual model of the factory could be made more sophisticated, first by allowing the cycle time to exceed 24 hours and estimating the consequences, and later to model and optimize teams of varying size for each of the manufacturing steps. This model is modified to address a few of the aforementioned limitations in the subsequent sections when applied to the AM core and reusable bagging materials concepts.

3.2 AM Core

For completeness the reader is referred to the first report in this series for a more in-depth overview of blade materials for conventional blades including sandwich cores, with section 3.1 introducing the NREL cost model.

3.2.1 Rationale

The rationale to produce sandwich cores via thermoplastic Additive Manufacturing within a blade factory revolves around flexibility in the manufacturing process, but also the ability to produce cores which have greater conformity to the curvature of the mould, this could enable a reduction in the number of hinge points or kerfs. This is important since this enables potential for larger core sections which conform to the mould and reduces the numbers of kerfs and thus in turn reduces the total resin uptake. Secondly the resin flow can be better controlled via bespoke resin channels at the surface of the core material.

3.2.2 Methodology

Additive layer manufacturing (ALM) involves moving a 3D printing head via a robot or gantry system to build up a part in layers. This approach will have benefits in that the part will be able to be formed so that it conforms to the blade surface without the use of kerf cuts, which as described in the previous section fill with resin and thus increase the mass and cost of resin required for the blade. The density of kerf cuts required varies with the local curvature of the blade and therefore the resin uptake also varies. The total mass of resin absorbed by the cores can be split into a part which is proportional to

the area of the core material which is related to cut cells and surface features to enhance resin flow and a part which is proportional to the volume of core material which is related to the kerf cuts made in the core material to allow it to conform to the mould.

Resin uptake in the core material was estimated from the bill of materials of the 83.5 blade of ORE Catapult's 7MW Levenmouth Demonstration Turbine (LDT). The shear webs have a surface area of 161.65m^2, volume of 5.14m^3 and absorb 582kg of resin, whereas the shells have a surface area of 336m^2, volume of 11.32m^3 and absorb 1210kg of resin. As the webs and the shells absorb the same amount of resin per square metre, we can assume that the assumption for both the webs and shells was 1.8kg/m^2. This is a simplistic approach which does not consider the resin absorbed by the volume of material into kerf cuts, so we have attempted to determine what resin quantity is likely to be absorbed.

Currently, blade manufacturers do not vary the quantity of kerf cuts with the local curvature of the blade. Core materials typically arrive pre-cut with kerfs to allow them to conform to the blade mould, and for the thick core materials used for blades a saw cut of around 0.9-1mm every 30mm would be typical [20].

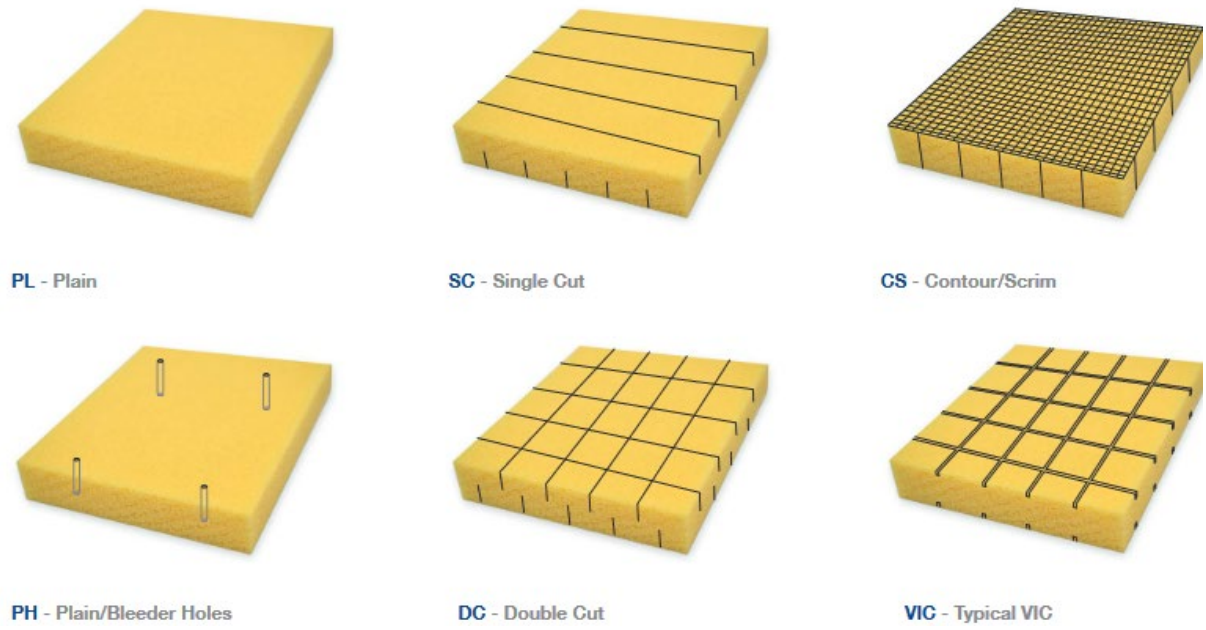

Figure 6 Types of core treatment available [20]

Depending on the application the core material will be finished in different ways as shown in **Error! Reference source not found.**. For wind turbine shells with double curvature, double cut (DC) as shown bottom-centre would be the chosen finishing method. The total mass of resin with density ρ_r absorbed into the core with density ρ_c, cut width w_c and spacing s_c can be calculated as shown below.

$$M_{kerf} = \rho_r w_c \frac{2t}{s_c}$$

Table 3 gives resin uptakes for a range of different core types and densities. We can use this information and the information from the Levenmouth Demonstration Turbine to check if the equation above is effective at calculating the total mass of resin absorbed. As previously stated, the calculation for the LDT appears to be done in terms of surface area only, so we are only aiming to match the overall quantities. Using the equation, we arrive at a quantity of 413kg of resin absorbed into the skin faces and 802kg of resin absorbed into the volume, for a total of 1215kg. The documentation for the LDT states that 1210kg of resin is absorbed into the PVC100/Balsa shell core materials so this equation appears to hold true. For the flat shear webs, it isn't necessary to kerf cut to the full depth, so something more like the vacuum infusion core (VIC) in **Error! Reference source not found.** would be typical. For this case, the cuts would only be 2mm deep and placed at a 20mm spacing. This value would be added to the surface area proportional part of the resin uptake.

$$M_{area} = M_{cut\ cells} + \rho_r w_c \frac{2d_c}{s_c}$$

Table 3 Core Types and associated resin uptake, from [20]

Type	Core Type and Density name	Panel Resin uptake (kg/m^2)
Gurit ® Corecell™ SAN	T300	0.94
	T400	0.56
	T500	0.46
	A500	0.49
	M60	0.84
	M80	0.71
	M100	0.61
	M130	0.55
	M200	0.49
Gurit ® PVC	PVC HT 80	0.62
	PVC 60	0.73
	PVC 100	0.56
	PVC 130	0.51
Gurit® Kerdyn™ (PET)	Kerdyn 80	1.09
	Kerdyn 100	1.04
	Kerdyn 115	1.01
	Kerdyn 135	0.96
	Kerdyn 150	0.93
	Kerdyn 200	0.81
	Kerdyn 250	0.7
	Kerdyn 300	0.58
Gurit® Balsaflex™ 150	12.5 mm Thick	1.7
	20 mm Thick	2.4
	25.4 mm Thick	2.7
	44.3 mm Thick	3.6

The total amount of resin absorbed is then found from the combination of these two factors. We should also factor in the mass of material which is removed when making the saw cuts and surface finishing features, so that if we are just attempting to characterise the total weight of the core plus resin we accurately account for the lost material.

If the core is created using additive manufacturing, then the weight can be calculated as follows. Additive manufacturing opens a host of possibilities, with many different combinations of parameters which can be varied to achieve the best properties, print rates and so on. This makes the problem fairly complex, but if we ignore for now the processing parameters and focus instead on the geometrical parameters, we can determine the range of parameters which allow an additively manufactured core to compete with a conventional core material in terms of weight.

These parameters are very simple, and there are only two of them:

- Effective wall thickness for perimeters and top and bottom layer - effective means that this wall thickness can be achieved by multiple thinner layers
- Infill density – this value is simply the ratio of the weight per volume of the material filling the part divided by the volume of the part to the material density if the part was solid

For the purposes of this work the additively manufactured core material panels will be treated as flat rectangular prisms with width w, length l, thickness t and effective wall thickness t_w. The infill density is v_f and the printing material density is ρ. The weight of a part can then be calculated as follows:

$$M = \rho(2t_w wt + 2t_w lt + 2t_w lw) + v_f \rho\big((l - 2t_w)(w - 2t_w)(t - 2t_w)\big)$$

This mass calculation was verified by using the AM slicing software 'IdeaMaker' to estimate the mass of AM prints and was found to hold true to within a few percent. Even if the infusion vacuum pressure does not cause material to get inside the watertight printed structure there will still be resin uptake into the skins of the panel just as there would be for a conventional core material because of the ribbed surface created as an artefact of the AM process. The amount of uptake will be a function of the bead size and layer height and can be estimated by assuming that the bead remains circular and the resin will be absorbed into the area between the top of the circle and its midline as shown in Figure 7.

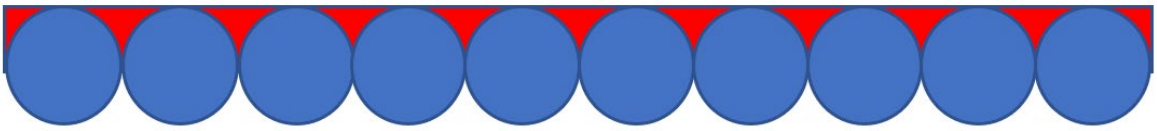

Figure 7 Assumption regarding resin absorption for AM cores.

In reality this should be a high-end estimate, as the layers will reduce in height and squeeze outwards and so should be somewhere between rectangular and circular. For a 1mm wall thickness and resin density of 1180kg/m3 this will result in 0.13kg of resin being added to each exposed face, or around one quarter of the conventional resin uptake of a PET core with density 100kg/m3 which would absorb 1.04kg of resin across both faces.

The AM core is heavier than a conventional core at low panel thickness because the heavier face skins are not offset by the elimination of resin material being absorbed into the kerf cuts. This trade off can be visualised as shown in Figure 8 for a 5mm infill density. The colour indicates the percentage mass increase (ranging from a reduction in mass of over 40% for a 140mm thick core with a 1mm wall thickness to an increase of over 100% for 20mm thick core with a 3mm wall thickness) and the red line indicates the break-even point with a conventional core in terms of overall mass (core material plus absorbed resin).

In reality, a 5% infill density is unlikely to be able to withstand vacuum pressure, and a 10% density will reduce the competitiveness with conventional core materials as shown in Figure 9. Beyond 10% infill density there are no core materials in the reference blade which are thick enough to allow the AM

core to beat a conventional core on infused weight, so a core with wall thickness of 1mm and an infill density of 7.5% will be used for future work.

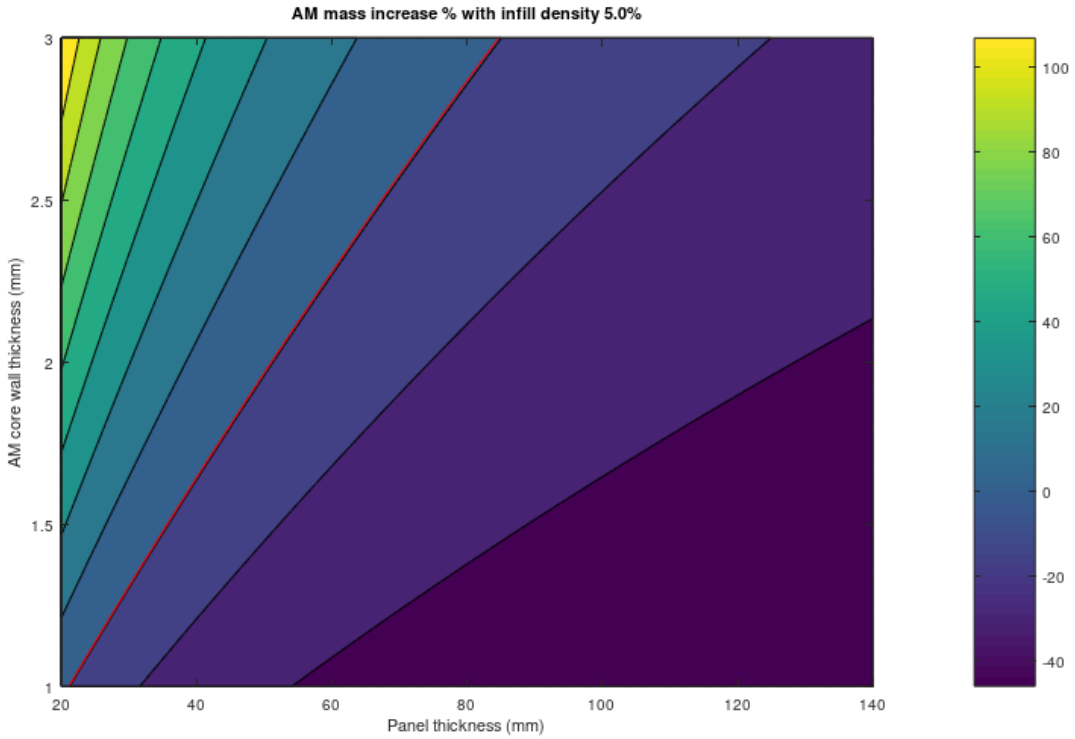

Figure 8 Percentage mass saving achieved by using AM core with 5% infill density.

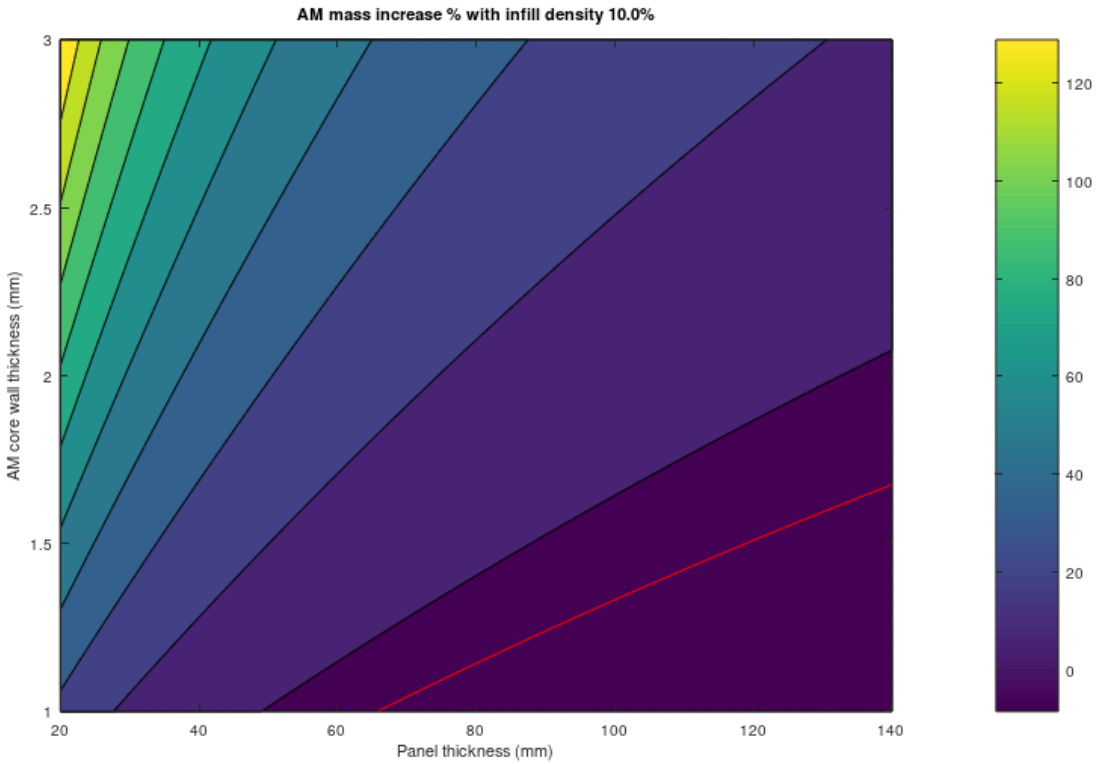

Figure 9 Percentage mass saving achieved with AM core with 10% infill density.

As the infill density has a strong bearing on the compressive and shear strength of the core material, it is very important to optimise the density so that it is high enough to withstand the infusion pressures and also to achieve the strengths required in service. The equivalent Young's modulus and compressive and shear strength are related to the volume fraction with a power law relationship as shown below (the exponent p will typically be around 1.8) so maximising the volume fraction is important – at 10% infill density the compressive strength will be around 3.5 times that at 5% infill density.

$$\tau_{v_f} = \tau_{100} C v_f^p$$

3.3 Costing of the Standard Infused Blade with Reusable Bagging Materials

This manufacturing variant will consider the use of the reusable silicon vacuum bag to determine how the use of reusable bagging materials might impact overall blade cost and the waste stream. The costing will be performed using ORE Catapult's implementation of the NREL Detailed Wind Turbine Blade Cost Model and where alterations were made to the standard cost inputs this will be highlighted. The following sections will describe how consumables, equipment and labour costs will be affected before presenting the results.

3.3.1 Consumables Cost

Consumables costs and wastes were determined from DFS Composites report from phase 1 of this work. Areal densities and material thicknesses were determined from [ref easycomposites.co.uk]. The consumables which are affected by the switch to silicon bags are shown in Table 4. The bagging film is not included in the NREL model, so it was included as layers in the blade model and then manually moved from materials to consumables after the cost modelling was completed. For the silicon bag model, the layer wasn't included, and the cost of tacky tape was set to 0.

Table 4 Consumables costs and mass

Consumable	Cost	Cost units	Thickness (m)	Areal weight (kg/m^2)	Density (kg/m^3)	Cost/kg ($/kg)
Tacky tape	0.24	£/m	-	-	-	-
Bagging film	0.61	£/m2	5e-5	0.055263	1105	12.47

3.3.2 Labour Costs

There are several labour steps in the NREL cost model which would be affected by the switch to silicon bags. These can be summarised as follows, along with their changes for the silicon bag model.

3.3.2.1 Application of Tacky Tape

This step originally had a lay down rate of 90m/hr/worker for the spars, webs and root and 360m/hr/worker for the shells. As this step is eliminated, the rate for all components was set to 1e10m/hr/worker to effectively eliminate the step for the silicon bag variant.

3.3.2.2 Application of the Vacuum Bag

The original rate of vacuum bagging was $7.5m^2$/hr for all components. As the bag is handled by a spreader beam and so can be draped across the entire part in one go, this process should be a lot quicker, but only one shell/web/spar can be done at a time because the crane will be in use for the process. For this reason, it has been assumed that the rate can be doubled to $15m^2$/hr.

3.3.2.3 Check of Vacuum Leaks

This step originally had a lay down rate of 30m/hr/worker for the spars, webs and root and 180m/hr/worker for the shells. The rates have been doubled to 60m/hr/worker and 360m/hr/worker respectively.

3.3.3 Equipment Costs

The reusable vacuum bag will shift the focus of costs from consumables to equipment. In addition to the cost of the bag itself, a spreader beam will be necessary to handle the bag and drape it over the blade mould.

3.3.3.1 Silicone Bag

Indicative properties for the silicone bag are shown in Table 5 – these have been obtained from the literature survey and by contacting various companies who make the bags [1].

Table 5 Properties of silicon bagging material

Property	Value	Units
Silicone density	1080	kg/m^3
Bag thickness	7	mm
Mass/area	7.56	kg/m^2
Cost/area	22	$\$/m^2$

The baseline blade developed in the previous Cornwall Flow Accelerator report was used for this analysis. The surface areas and estimated bag weights and costs for each component of the blade are shown in Table 6.

Table 6 Vacuum bag properties for various components

Component	Surface Area (m^2)	Bag Mass (kg)	Bag Cost ($)
Pressure side shell	629.0	4755.2	13,838
Suction side shell	633.3	4787.7	13,932
Pressure side spar cap	111.4	842.2	2,450
Suction side spar cap	111.3	841.4	2,448
Web 1	211.6	1599.7	4,655
Web 2	207.5	1568.7	4,565
Root preform	132.0	997.9	2,904

As the life of the bag is not known, three scenarios have been considered – one where the bag will survive for 30 pulls, one where it survives for 150 pulls and one where it survives for 300 pulls. The equipment variable for the infusion process has been modified for each of these cases, amortising the total cost of bags over 10 years (the lifetime of the rest of the infusion equipment). As the equipment

costs for infusion scale with the characteristic length of the component, the total cost of infusion equipment has been divided by the characteristic length for each number of pulls.

3.3.3.2 Spreader Bar

As the spreader bar is extremely long and lifting a relatively small load, a truss structure has been selected to minimise steel requirement. There is a trade-off here between the higher labour cost of making a truss structure compared to a box-beam, but given the current high steel costs a truss structure was a better option. Also, similar tools (for example shear web handling tools) utilise truss structures. The beam is assumed to be made from S355 steel, and a safety factor of 4 has been used for lifting apparatus [19]. The design process for the spreader bar (visualised in Figure 10) was as follows:

1. Calculate the mass per unit area of mould surface
2. Estimate the intervals at which the bags would need to be supported. As the material property data available for the bag materials did not include enough information to model the possible support spacing, a spacing of 4m was used which appeared to be consistent with videos showing the use of reusable silicon bags online
3. Calculate the required length of the outriggers which will support the bag in the chordwise direction
4. Calculate the required steel mass for the outriggers to support the bag plus the self-weight of the outrigger beams
5. Add the outrigger beam mass to the mass of the bag and use this value as a distributed load on the main beam structure
6. Select a truss height and width, and tube diameters and wall thicknesses.
7. Use ANSYS SpaceClaim script to generate the nodal positions and beam elements for the model
8. Perform nonlinear large deflection analysis with ANSYS Mechanical (element size 0.2m using BEAM188 elements)
9. Calculate maximum combined stress using the beam tool in ANSYS Mechanical and ensure it is below 88MPa (355MPa with a safety factor of 4)
10. Evaluate deflection and ensure it is not greater than 1/500 beam length
11. Perform eigenbuckling analysis using nonlinear static structural as the pre-stress environment and ensure the buckling margin is OK
12. Iterate 6-11 to minimise mass

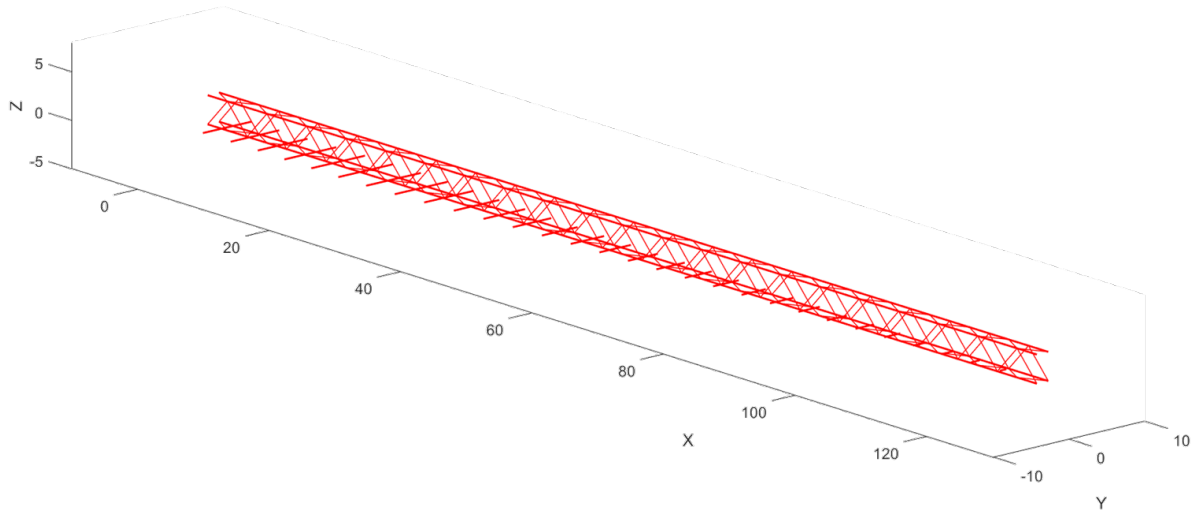

Figure 10 Silicone bag handling beam.

The space frame design aimed to use standard tube sizes. After iterating the design to satisfy the stress, deflection and buckling constraints the longitudinal members are 114.3mm in diameter with a 3mm wall thickness, and the reinforcement members are 60.3mm diameter with a 3mm wall thickness. Model loads and boundary conditions are shown in Figure 11, the maximum direct stress is shown in Figure 12 and Figure 13 shows the deflection of the beam due to its self-weight and the weight of the vacuum bag. The buckling margin was found to be 1.7.

The resulting structure weighs 6.2t, plus the weight of the outriggers which total 2.13t. Current costs for fabricated steel structures of this type are in the region of £8/kg, so each spreader tool would cost around £67k. As no detail design has been performed on the structure to increase detail around the points of load application and account for other fixings etc, we will assume a total cost per beam of £80k.

As the factory layout is such that webs, spars and shells are all manufactured in different areas we can assume that 3 beams are required – one to operate in each part of the factory. The life of the beam can be assumed to be 10 years (the same as the rest of the infusion equipment).

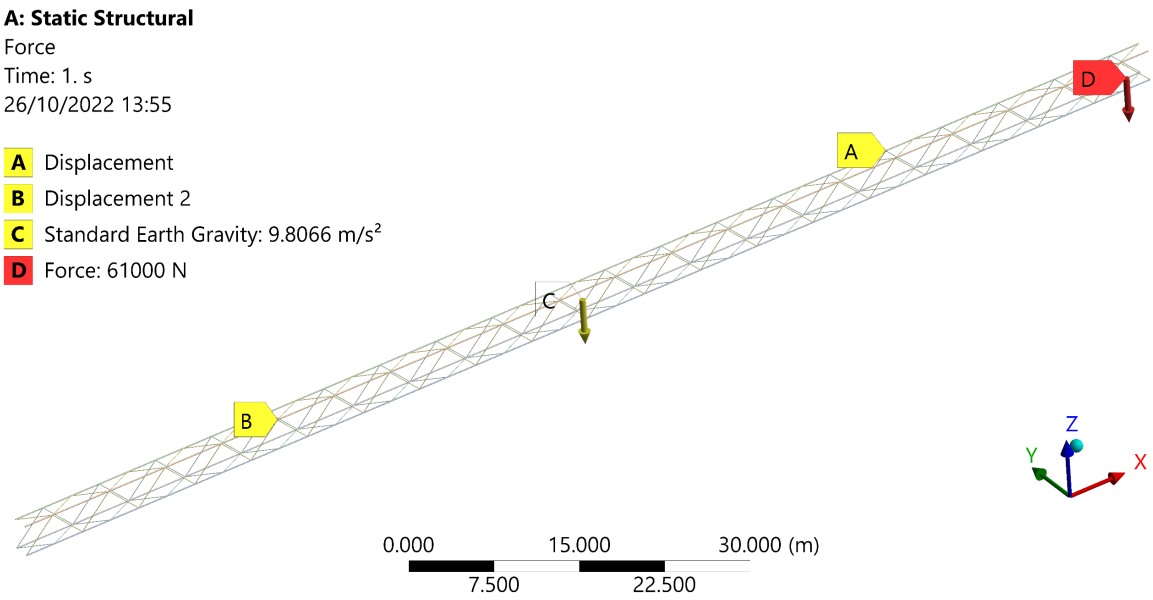

Figure 11 ANSYS Simulation loads and boundary conditions.

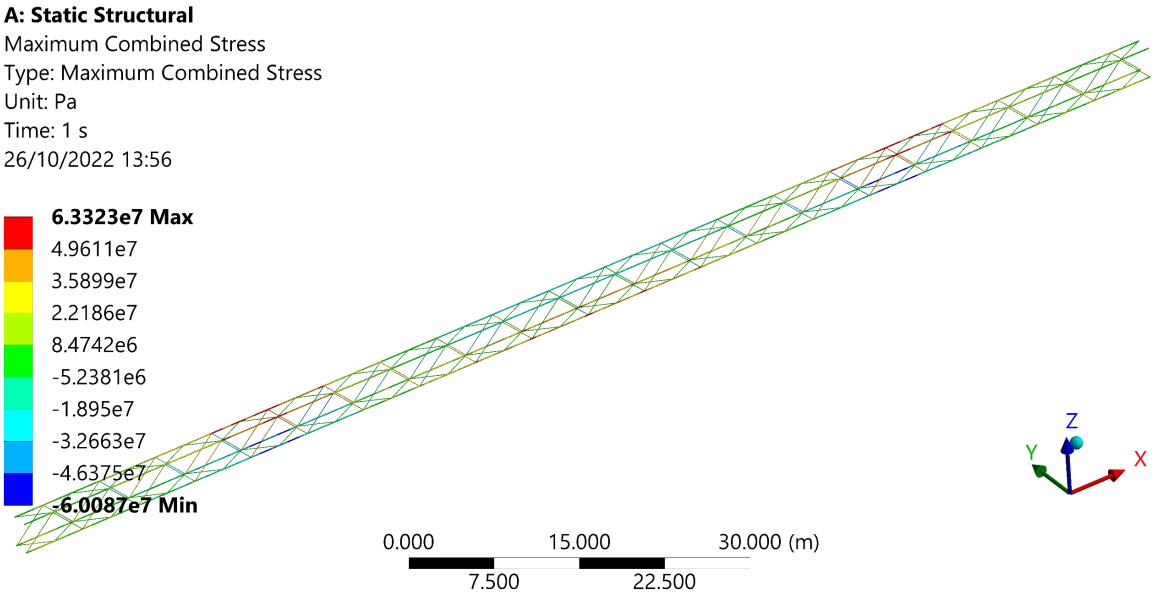

Figure 12 Maximum combined stress in structure

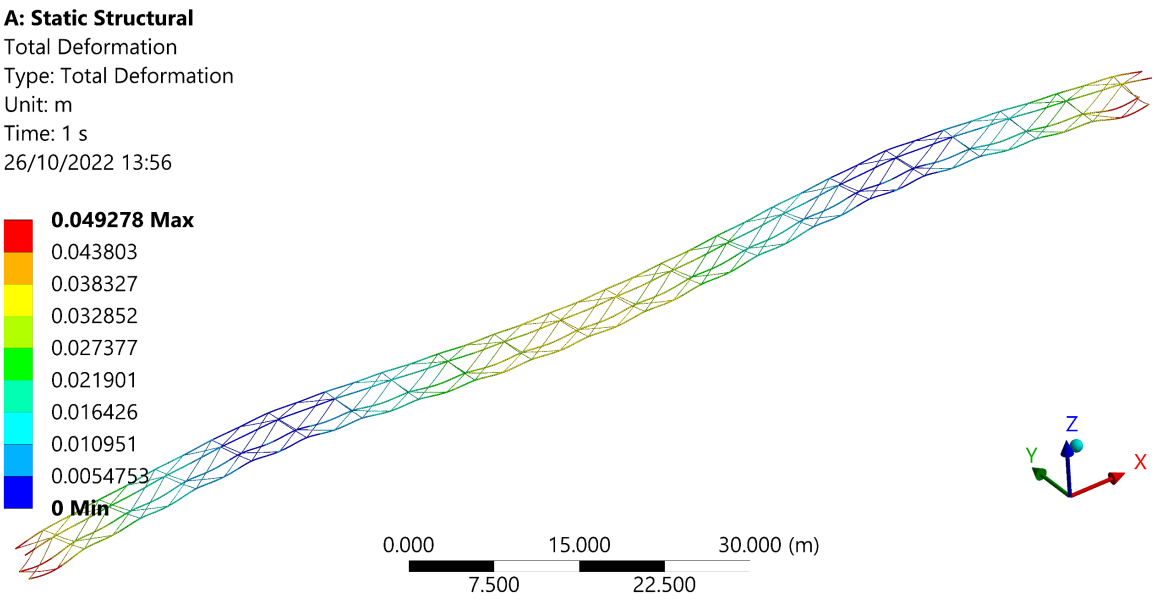

Figure 13 Deflection of spreader beam

3.3.4 Results

The 4 cost model results are compared in Table 7. Even if it only survives for 30 mould pulls, the silicone bag shows a cost benefit – however it is important to note that with this lifetime the duration for which the mould would need to be out of action to spray up a new silicon vacuum bag would become significant (this has not been accounted for in the current costing). Also, at 30 mould pulls, the mass of waste vacuum bags (15,392 kg) would be greater than the mass of bagging film which it replaces (105 kg x 30 blades is 3,150 kg). Even at 150 pulls the benefit is marginal (around 400 kg), but at 300 pulls there is a clear benefit in terms of mass of material going to landfill.

There is a large increase in equipment costs and associated maintenance costs for the 30-pull bag, but this is offset by reductions in labour, overheads and, of course, consumables. The reductions in utility costs, tooling costs and building costs can be explained by the fact that we have not forced the model to round up to an integer number of processes (to avoid masking small changes in process time with big jumps occurring from rounding up to the next number of e.g., skin moulds). This means that the reduction in labour time has allowed fewer parallel processes and therefore less floor area (which leads to lower building costs, which means less area to light, hence lower utility costs) and fewer moulds to process the same amount of blades (hence lower tooling costs).

In order to justify the high up-front cost more work would be necessary to understand how many cycles the bags can last for as this is clearly extremely important for both the business case and the environmental case.

Table 7 Main Results Comparison

Cost Element	Baseline	Silicon Vacuum Bag (30 pulls)	Change (%)	Silicon Vacuum Bag (150 pulls)	Change (%)	Silicon Vacuum Bag (300 pulls)	Change (%)
Materials	$600,090	$600,089	0.0%	£600,090	0.0%	£600,090	0.0%
Consumables	$11,180	$9,521	-14.8%	£9,521	-14.8%	£9,521	-14.8%
Labour	$124,375	$118,678	-4.6%	£118,678	-4.6%	£118,678	-4.6%
Overheads	$37,312	$35,603	-4.6%	£35,603	-4.6%	£35,603	-4.6%
Utility Costs	$97,427	$93,766	-3.8%	£93,767	-3.8%	£93,767	-3.8%
Equipment Costs	$6,341	$11,256	77.5%	£7,385	16.5%	£6,901	8.8%
Tooling Costs	$16,837	$16,382	-2.7%	£16,382	-2.7%	£16,382	-2.7%
Building Costs	$1,560	$1,517	-2.7%	£1,518	-2.7%	£1,518	-2.7%
Maintenance Costs	$7,102	$8,945	26.0%	£7,396	4.1%	£7,203	1.4%
Cost of Capital	$17,742	$20,282	14.3%	£18,052	1.8%	£17,773	0.2%
Total	$919,966	$916,043	-0.4%	£908,393	-1.3%	£907,436	-1.4%

3.4 Alternative Blade Materials

Alternative environmentally friendly materials have been identified and investigated in this work that could potentially meet blade performance requirements. The environmental and economic impact of the use of the "new" materials was assessed based on quantitative and robust methodologies whilst feasible optimized blade designs with minimum CO_2 footprint were possible to be produced.

This section focuses on ORE Catapult activities, that is the structural design and optimization of the wind turbine rotor blade. More specifically, the in-house, advanced blade design tool ATOM [2], [3] and [4] is presented in the next sections. Furthermore, the identified new materials are listed along with a description of their deployment in the various regions of the blade. The set-up of the optimization process for the various "alternative material" blade designs is presented and discussed. Useful conclusions are derived regarding the effective deployment of the environmentally friendly materials and the corresponding blade and CO_2 mass savings on each blade design compared to the baseline one.

3.4.1 Methodology

The structural design of the blade using alternative materials was performed using ATOM (Aeroelastic Turbine Optimisation Methods). ATOM co-developed under the Wind Blade 23 Research Hub (WBRH) by the Offshore Renewable Energy Catapult and Bristol University. It is an analysis and optimisation tool specifically aimed at the optimisation of aeroelastic tailored, horizontal-axis wind turbines whereby turbine topology remains fixed during the optimisation. From an analysis point of view, a set of numerical design variables (DVs) that define each aspect of a turbine can be input by the user, ATOM then performs every step from meshing of the blade and tower beams, right through to running a full set of aero-servo-elastic design load cases (DLC) and post-processing results for statistics on power, loads, cross-sectional strains, and failure indices. This analysis capability is smoothly integrated within an optimisation framework with a choice of algorithms.

A key feature of ATOM's design capabilities is the use of spline surfaces and lamination parameters [2]. During optimisation, DVs control a number of spline surfaces that define variations in lamination parameters and laminate thickness across the blade. This framework allows for the optimisation process to be unconstrained by conventional structural configurations and stacking sequences. ATOM utilises a range of analysis modules, a brief summary is given here:

- The aerodynamic model utilises a modified blade element momentum theory with corrections for dynamic wake and dynamic stall.
- The structural models of the blade and tower utilise beam finite-elements, with linear damping. The beam elements allow for anisotropic composite laminates with fully populated stiffness and mass matrices. A cross-sectional modeller uses 2D bar elements to generate properties from the laminate spline surfaces. ATOM allows for high-order beam modelling whereby three, four or five node beam elements can be used.
- The non-linear aero-servo-elastic model combines aerodynamic and structural models with a simple controller and multiple options for time-varying wind fields. The controller is embedded into the code and employs PI pitch control above rated and a simple optimal mode gain to control torque below rated.
- The optimisation algorithm implemented is the globally convergent method of moving asymptotes (GCMMA) [5]. GCMMA uses the function values and gradients at each step to generate a convex subproblem that approximates the real objective and constraint functions. If the solution to the subproblem is found to be inaccurate when checked against the real values, then the approximating functions are sequentially modified until they are conservative, resulting in an improved and feasible solution.

There are two main architectures to solve multi-disciplinary optimisation (MDO) problems like the one of the designs of a wind turbine rotor blade, that is, the monolithic and distributed architecture. Monolithic architecture considers the whole problem in a single optimisation procedure. All the analysis modules are combined to produce a single set of objective and constraint functions and all of the DVs are present in a single optimisation. Monolithic architectures have the advantage of being simpler to implement as they typically mimic conventional analysis workflows whilst they can consider all the interactions/couplings of the different aspects involved in the analysis for example aerodynamic

and structural one. However, the computational cost of monolithic architectures is high. In contrast to monolithic architectures, distributed architectures decompose the MDO problem into a number of smaller sub-problems. That is, the aerodynamic and structural design is separated into two sub-optimisation processes. In ATOM, the user has the capability to simulate either adopting a monolithic approach, in the frame of this work called “aero-structural” optimisation approach or using a distributed architecture called “frozen load“ optimisation approach. Herein, due to the high computational cost of an “aero-structural” optimisation as well as the large number of different materials to be investigated, the “frozen load” approach was adopted. In “frozen load” optimisation loop, an initial calculation of aeroelastic loads for an initial non-optimised blade design is performed. Having calculating loads, the structure is optimised. For the new optimised structure, new loads are evaluated. The loop continuous until convergence of specific metrics, e.g. tip displacement or blade frequencies. Based on previous experience, “frozen load” optimisation although it is not guaranteed that will converge, nevertheless it can give acceptable results, close to the ones obtained from an “aero-structural” optimisation approach with less computational effort.

It is important to say that a constrained optimization problem is about to find the minimum (or the maximum) of a function, usually named the objective function whilst some constraints should be satisfied. The objective function in the rotor blade design context could be the mass of the blade or the Levelized Cost of Energy (LCoE) of the wind turbine machine. For the constraint requirements, these could be that any stress developed at any point in any section of the blade to be less than the allowable stress of the material or the tip displacement of the blade to be less than the distance between the tip and the tower. An optimization algorithm searches the design space in an automatic and efficient way to find minimum (or maximum) of the objective function. The starting point (initial design) is crucial for gradient based optimization algorithms as the ones implemented in ATOM. It determines whether the algorithm will converge to a local or a global minimum as depicted in Figure 14.

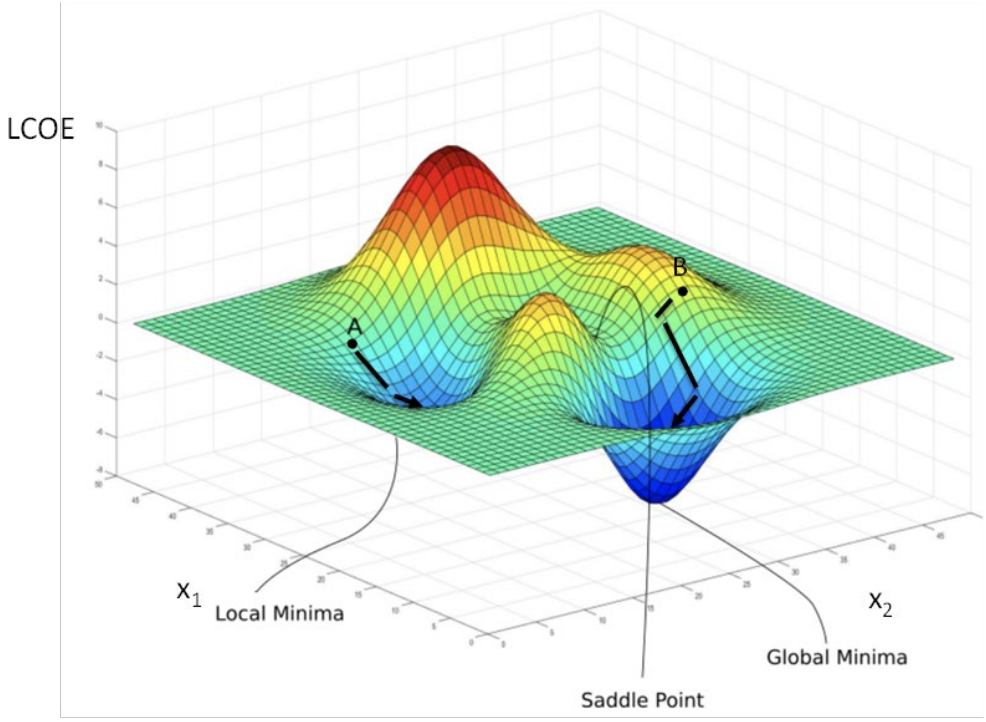

Figure 14 Arbitrary objective function in the design space.

If the initial design point is located at point A, then the most probable scenario would be the optimization algorithm to be trapped in the nearest trough. A completely different outcome would be produced, if point B was selected as the starting point. In the context of this work, every time that the materials in the blade change, the shape of the surface (or the objective function) changes and thus, finding the global minimum which is the main target is not an easy task whilst it is not guaranteed. Although there are optimization algorithms that can search and find the global minimum, nevertheless their implementation to optimise blade structures would be in vain due to the extremely high computational cost.

In this work, the objective function of the optimisation problem was set to be a modified LCoE that considers the CO_2 footprint from cradle to gate of every material. More specifically, ATOM uses a cost model to estimate capital and operational expenditure costs (CAPEX and OPEX respectively) and finally to estimate the LCoE of the wind turbine machine analysed. It is assumed that only the material cost is important when comparing different blade designs that only the materials change (if the cost of the technology to fabricate the blade remains the same). Making one step forward and trying to include CO_2 mass of each material in the blade optimisation process, the material cost, for example £X per [kg] of material in the cost model, was replaced by the generated mass of CO_2 in [kg] per [kg] of each material. The modified LCoE essentially sets the optimization algorithm to search for the minimum Global Potential Warming (GWP) value of the blade. The trade off in this new optimisation framework is between performance and environmental impact of the blade. Materials with adequate mechanical properties and smaller GWP values will be favoured by the optimisation algorithm.

Design constraints imposed in the blade optimisation of this work are related to strength, buckling, fatigue, tower clearance and aeroelastic stability of the blade as well as some manufacturing constraints related to the taper of the composite plies and the core materials.

Regarding the DVs, only variables that affect the internal structure of the blade were considered, that is, the thickness of the various layers along the length of the blade structure. The normalised location of the spline control points along the blade length (each one corresponds to one DV) are presented in Table 8.

Table 8 List of design variables

Name	#DVs	Normalised location of spline control points along the blade arc-length. 0:Root, 1: Tip	Comments
Shell UD	10	[0 0.02 0.05 0.1 0.25 0.4 0.6 0.8 0.9 0.95]	Baseline: glass
Shell Biax	10	[0 0.02 0.05 0.1 0.25 0.4 0.6 0.8 0.9 0.95]	Baseline: glass
Spar UDc (pressure side)	8	[0.05 0.1 0.25 0.4 0.6 0.8 0.9 0.95]	Baseline: carbon
Spar UDc (suction side)	8	[0.05 0.1 0.25 0.4 0.6 0.8 0.9 0.95]	Baseline: carbon
Spar UDg	8	[0.05 0.1 0.25 0.4 0.6 0.8 0.9 0.95]	Baseline: glass
Web Biax	8	[0.04 0.1 0.25 0.4 0.6 0.8 0.9 0.96]	Baseline: glass
Web core	8	[0.04 0.1 0.25 0.4 0.6 0.8 0.9 0.96]	Baseline: foam
LE UD	5	[0.1 0.25 0.4 0.6 0.8]	Baseline: glass
LE core (suction side)	7	[0.1 0.25 0.4 0.6 0.8 0.9 0.95]	Baseline: foam
TE UD	5	[0.1 0.25 0.4 0.6 0.8]	Baseline: glass
TE core (suction side)	7	[0.1 0.25 0.4 0.6 0.8 0.9 0.95]	Baseline: foam

A reduced set of IEC design load cases [6] —1.1 and 1.3— were examined as these have been found to offer a good estimate of ultimate blade loads without excessive computational effort [7].

The baseline design has been analysed and optimised in a previous task of this project whilst it has been thoroughly described in [7]. The initial design point for all the different designs that has been examined when changing materials is based on the optimised baseline blade design.

3.4.2 Alternative Resin Materials

Several environmentally friendly materials were examined in this work both for the fibre and the matrix constituent of the composite lamina. More specifically, regarding matrix materials, a bio-based epoxy (InfuGreen810) [8], a thermoplastic (Elium180) [9] and a vitrimer recyclable thermoset (Vitrimax) resin [10] were examined due to either their recyclability or their lower GWP value compare to standard epoxy resin systems. The various material systems that form the lamina/laminates in the blade structure were composed by one of the environmentally friendly resins mentioned above and E-glass fibres. A detailed description of the matrix materials is presented in the following sections. Indicative mechanical property average values and GWP values of a unidirectional lamina (UD) and biaxial laminate of an E-glass/alternative resin material system are listed in Table 9 and Table 10

respectively. Strength material properties for the biaxial laminates were assumed like the UD ones. It is highlighted that material properties at the lamina (or laminate) level presented in Table 9 and Table 10 were derived using micro mechanical models, for example rule of mixtures. To be as realistic as possible, appropriate knockdown factors, listed in Table 11, were assumed and applied to the material properties to consider the effect of various sources of uncertainties that are not present when experimentally deriving material property values. An additional knockdown factor could be possibly introduced to consider the effect of model uncertainty related to the estimation of the property values using micromechanical models, but this is out of the scope of this work, and it was not further examined.

Table 9 Material properties for a UD lamina made of alternative resin materials (E-glass/alternative resin)

	Bio-based (InfuGreen810)	Thermoplastic (Elium180)	Recyclable resin (Vitrimax)
V_f [%]	53.5	53.5	53.5
E_1 [Mpa]	43218	43204	43358
E_2 [Mpa]	15364	15208	16938
ν_{12}	0.28	0.29	0.28
G_{12} [Mpa]	3102	3188	3343
X_T [Mpa]	1105	1105	1109
X_C [Mpa]	621	634	620
Y_T [Mpa]	68	66	80
Y_C [Mpa]	86	116	85
S [Mpa]	43	43	43
rho [g/cm^2]	1.90	1.87	1.89
GWP [kg CO_2eq/kg laminate]	2.44	2.12	2.54

Table 10 Material properties for a biaxial ±45 laminate made of alternative resin materials (E-glass/alternative resin)

	Bio-based (InfuGreen810)	Thermoplastic (Elium180)	Recyclable resin (Vitrimax)
E_1 [Mpa]	10519	10773	11277
E_2 [Mpa]	10519	10773	11277
G_{12} [Mpa]	12853	12776	13104
ν_{12}	0.70	0.69	0.69
GWP [kg CO_2eq/kg laminate]	2.44	2.12	2.54

Table 11 Knockdown factors applied to the material property values of UD lamina and biaxial laminates

	UD	BIAX
E_1	0.95	0.97
E_2	0.97	0.97
G_{12}	0.97	0.97
X_T	0.82	0.82
X_C	0.85	0.85
Y_T	0.91	0.91
Y_C	0.95	0.95
S	0.96	0.96

3.4.2.1 Bio-based epoxy (InfuGreen810)

The bio-based epoxy system that was examined in this work is the InfuGreen810 system. It is a "green" epoxy specially formulated for resin transfer processes such as injection and infusion. This system has a very low viscosity at ambient temperature and thus make it ideal to be used in resin transfer processes. The cured system gives a temperature resistance up to 100°C. The different hardeners allow the production of small to very large parts. More specifically, the hardeners SD 4770 and 4771 are designed for very thick laminates by infusions. This is a desirable feature when making large rotor blades (especially near to the root of the blade). InfuGreen 810 Epoxy resin is produced with about 38 % of carbon from plant origin and has a lower environmental impact than standard Epoxy systems.

3.4.2.2 Thermoplastic (Elium180)

Elium180 is a liquid thermoplastic resin for infusion and resin transfer mould processes at ambient (or elevated) temperature to produce thermoplastic continuous fibre composite reinforcements. Due to low viscosity of the resin at room temperature, the same low-pressure processes and similar equipment's used today to process thermoset composite parts can be used. Therefore, Elium180 is a matrix material that can be used in blade manufacturing without requesting new technologies and thus, additional capital costs. The resulting thermoplastic composite parts show mechanical properties similar to those parts made of standard epoxy resins whilst presenting the major advantages of being post-thermoformable and recyclable.

3.4.2.3 Vitrimer recyclable thermoset (Vitrimax)

Vitrimer resins (Vitrimax) enable circularly recyclable composite structures, and the option of post-cure processing provides high manufacturing flexibility. Like standard thermoset prepreg resins, Vitrimax resins come in 2 parts which can be mixed and applied using standard prepreg practices. Once cured, these materials produce highly crosslinked network polymers for structural stability. However, unlike traditional thermoset prepreg, VITRIMAX resins enable post-cure processing to change shape. After impregnation, the prepreg can be partially or fully cured for extended shelf life at room temperature and reduced in-mould time during production. VITRIMAX relies on Tg-dependent covalent chemical bond welding at the surface of laminates that creates a fully crosslinked thermoset and resultant stability. Unlike thermoplastic prepreg, VITRIMAX does not require long melting and cooling periods for part production, simply heat to the defined Tg range to activate bonding.

3.4.3 Alternative fibre materials

Several natural fibre materials were investigated in this work, that is, mineral fibres like Basalt fibres [11] and plant fibres such as Jute [12], Hemp [13] and Kenaf [14]. They were explored and assessed whether they can be deployed in a rotor blade without compromising performance. The various material systems that form the lamina/laminates in the blade structure were composed by one of the environmentally friendly fibre materials mentioned above and a standard epoxy resin. A detailed description of the fibre materials is presented in the following sections. Typical mechanical property average values and GWP values of a unidirectional lamina (UD) and biaxial laminate of the alternative fibre/epoxy material system are listed in

Table 12 and Table 13 respectively. Strength material properties for the biaxial laminates were assumed similar to the UD ones. It is highlighted that material properties at the lamina (or laminate) level presented in

Table 12 and Table 13 were derived using micro mechanical models, for example rule of mixtures. To be as realistic as possible, appropriate knockdown factors, listed in Table 11, were assumed and applied to the material properties to consider the effect of various sources of uncertainties that are not present when experimentally deriving material property values. Academic studies on the comparison in cost per weight of the fibres [13], illustrated that the unit price of most natural fibres is lower than that of glass and carbon fibres.

Table 12 Material properties for a UD lamina made of alternative fibre materials (alternative fibre/epoxy)

	Glass	Basalt	Jute	Hemp	Kenaf
V_f [%]	53.5	53.5	53.5	53.5	53.5
E_1 [Mpa]	41214	50173	22888	31849	19544
E_2 [Mpa]	14883	15185	16786	15874	17457
v_{12}	0.28	0.27	0.27	0.27	0.27
G_{12} [Mpa]	3019	3130	2636	2872	2509
X_T [Mpa]	905	1158	229	328	334
X_C [Mpa]	527	651	156	210	207
Y_T [Mpa]	59	65	65	65	65
Y_C [Mpa]	81	85	85	85	85
S [Mpa]	41	43	43	43	43
rho [g/cm^2]	1.96	2.00	1.33	1.33	1.30
GWP [kg CO_2eq/kg laminate]	2.90	2.77	2.19	1.88	2.13

Table 13 Material properties for a biaxial ±45 laminate made of alternative fibre materials (alternative fibre/epoxy)

	Glass	Basalt	Jute	Hemp	Kenaf
E_1 [Mpa]	10190	10733	8749	9600	8349
E_2 [Mpa]	10190	10733	8749	9600	8349
G_{12} [Mpa]	12510	14612	8085	10157	7374
v_{12}	0.70	0.71	0.66	0.67	0.66
GWP [kg CO_2eq/kg laminate]	2.90	2.77	2.19	1.88	2.13

3.4.3.1 Basalt fibres

Basalt fibre is similar to carbon and glass fibres, but basalt has better mechanical properties than glass fibres and is lower in cost than carbon fibre. Basalt fibres exhibit some attractive feature such as: high strength and high modulus, excellent shock resistance, high temperature resistance and good light resistance, good fatigue and corrosion resistance properties, no need for special processing equipment, easy to handle and process and environment friendly (basalt-reinforced composites can meet OEM's disposal requirements because complete disposal by incineration is possible. They can be recycled). They exhibit no health and safety risks. They are compatible with many resins - unsaturated polyester, vinyl ester, epoxy, phenolic and they offer better chemical resistance than E-glass fibres.

3.4.3.2 Jute fibres

Jute woven fabrics are reinforcement textiles based on natural jute fibre and designed for fibre reinforced polymer composite applications. Jute offers the benefits of premium natural fibres such as flax – including a favourable stiffness-to-weight ratio – but at a lower cost compared to glass fibres. The fabrics can be processed in a similar way to glass or carbon fibre and are suitable for use with a wide variety of resins, including synthetic and bio-based systems. Typical processes include wet lay-up, vacuum infusion and resin transfer moulding making it suitable for the manufacture of wind turbine blades.

3.4.3.3 Hemp fibres

Hemp fibres are very strong whilst the plant that gives hemp can grow faster than other natural fibres plants. Hemp fibres are recyclable, non-toxic, and biodegradable materials and exhibit excellent specific stiffness properties. On the negative side of the industrial hemp is that it is restricted the growth and cultivation of this plant in many countries around the world.

3.4.3.4 Kenaf fibres

Kenaf fibres have been investigated in the past and very good mechanical properties have been reported. The specific stiffness is comparable to the glass fibre ones and the price is 3 to 2 times lower than of the glass fibres. The elongation at failure is also comparable to that one of glass fibres. Thermoplastic and thermosetting matrices have been used to produce kenaf fibres reinforced composites. A positive effect of specific agents on the bonding and the wettability of kenaf fibres was reported. The pre-treatment of the fibres improves the mechanical properties of the composite. Kenaf is a plant that grows fast so potentially high volumes of the Kenaf plant could be produced for further use. On the negative side, it demands high water requirements for growth as well as the handling and processing of long fibre bundles is difficult. The standard laminating epoxy resins are suitable for manufacturing of kenaf fibre reinforced laminated bio-composites with useful engineering properties. Kenaf fibres composite can be produced using conventional fibre composite manufacturing methods.

3.4.4 Material deployment

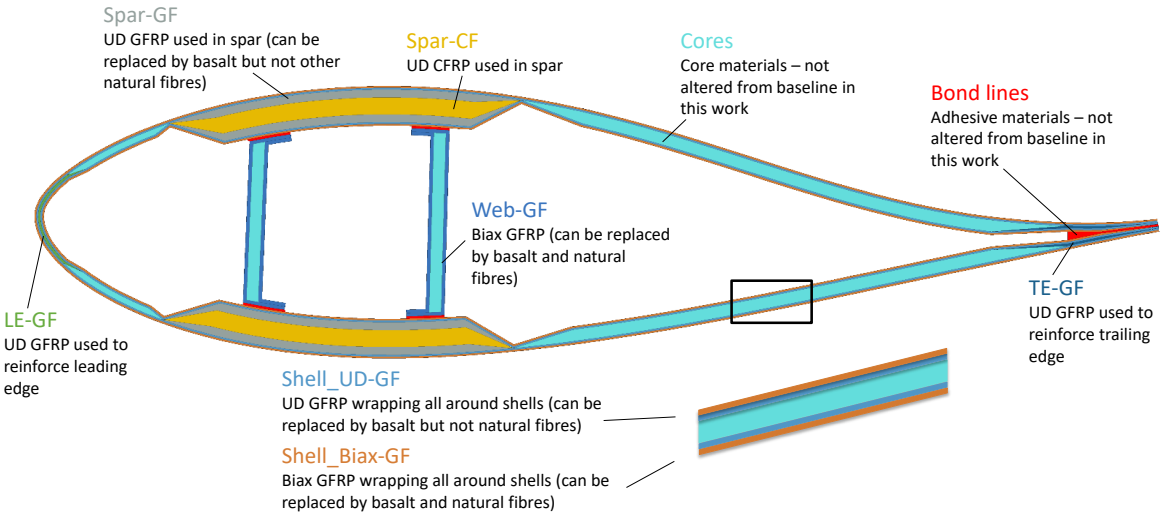

Figure 15 Blade section with material deployment.

The replacement of standard fibre materials, for example carbon or glass fibres, with natural fibres needs a careful consideration from a structural point of view in the blade. From Table 12 to Table 13, it is obvious that natural fibre materials, generally, present inferior mechanical properties compared to glass (or carbon) ones. An exemption to this trend is the basalt fibres which compared to glass fibres they seem to perform better. Examining, however, the specific properties of the natural fibres, that is their stiffness and strength properties divided by their density then plant based natural fibres exhibit excellent specific stiffness properties compared to the ones of the glass fibres. Strength specific properties in the longitudinal direction are still inferior to the respective properties of the glass fibres, not however, the transverse and in plane shear strength properties. Different trend is presented by Basalt fibres in which it is superior to the longitudinal direction but not in the transverse and the in-plane shear direction. Therefore, one promising action for plant based natural fibres would be to replace standard materials in those areas of the baseline blade design that stiffness was the main design driver. These are mainly the areas of the blade that sandwich laminates exist. Additionally, areas in which design driver could be possibly the shear strength, e.g., the webs of the blade, should be preferred and glass material could be replaced with the new environmentally friendly materials.

Regarding matrix materials and with reference to Table 9 to Table 10, new resins offer improved material properties compared to the respective standard epoxy resin systems. Both specific strength and stiffness properties are slightly better than the ones of a typical E-glass/epoxy system and thus, could replace glass fibre materials in a broader region of the blade compared to natural fibres.

As a starting point in this work, the biaxial glass laminates of ±45 fibre orientation relative to the blade length were mainly replaced with the new plant-based fibre materials. Biaxial laminates exist at the skins of the sandwich laminates in the shells and webs of the blade. Exemption to this approach was when basalt fibres were used. In this case, all the UD and biaxial laminates of glass fibres in the skin,

webs and spar caps were replaced with the basalt ones. Nevertheless, it is recognized that replacing glass biaxial layers in shell and webs is a risky step considering the inferior in-plane and transverse specific properties of Basalt fibres. But, as already mentioned, this work comprises the first step toward understanding the performance of these new environmentally friendly materials. For the matrix materials, they substitute the glass UD and biaxial laminates in shells, spar caps and webs of the blade due to the better specific properties of these resins. A typical blade cross section along with its components and typical materials are depicted in Figure 15. A thorough description has already been given in [7] for the baseline blade design. A summary is reported herein to highlight the deployment of the new materials. This deployment is also captured in Figure 15.

More specifically, the outer geometry of a blade is typically formed by the assembly of two half shells to give it an aerodynamic shape. Each half shell is a sandwich construction of fibre-reinforced polymer composite skins on either side of a low-density core material as shown in the detail of the figure. The skins in the baseline blade design were made of UD glass material and biaxial laminates of ±45 fibre orientation relative to the blade length. The biaxial glass laminates were replaced with biaxial laminates made of all the plant-based fibre materials. In case of basalt fibres both UD and biaxial laminates were replaced with the new material.

The spars that carry the main loading and are heavily stressed components are made using hybrid glass/carbon fibres. UD glass material was replaced only from basalt material. No plant based natural fibre materials were used to replace UD glass plies due to their inferior mechanical properties and the fact that the spars are highly stressed components.

Webs that are the vertical components in the section and take shear loading are made as composite sandwich plates with low density core and biaxial glass laminates. The biaxial layers were replaced with the suggested alternative materials.

Finally, glass UD layers are used to the leading edge (LE) and trailing edge (TE) areas of the blade to give stiffness in the edgewise direction. No replacement was decided for any material in these areas.

3.4.5 Blade design comparison using the alternative materials

Simulations were performed in ATOM with parameter settings as described in section 3.3.1. One simulation concerned the optimisation of the baseline design with respect to the modified LCoE. Seven simulations were followed corresponding to the alternative materials investigated in this work (i.e., Basalt, Jute, Hemp, Kenaf, Bio-epoxy, thermoplastic and Vitrimer). Results for the seven design cases are depicted in

Figure 16. More specifically, the percentage of change of the blade and CO_2 mass with respect to the corresponding ones of the baseline design is displayed with dark and light blue colour bars in

Figure 16 respectively. The annual energy production (AEP) was found to be similar for all the blade designs and approximately equal to 7.96E+10 Wh. This trend of the unchanged AEP value was mainly

attributed to the specific set up of the optimisation process in which design variables related to the external geometry of the blade were not considered. Thus, the planform for all the different blades kept the same and only the thickness of each laminate at the various station along the blade length was modified.

With reference to

Figure 16, all the suggested materials drive the mass of the blade down although, in the optimization process, the modified LCoE was defined as the objective function and not the blade mass. That is, the optimization algorithm was set to identify the minimum CO_2 mass production for each blade instead of the blade mass itself. Therefore, it is on the positive outcomes of this work that attempting to minimize the CO_2 footprint of the baseline blade can result in at the same time lighter blade designs. In

Figure 16, mass reduction of up to 11.3% is observed for the Hemp fibre material. All the plant based natural fibre materials perform quite well. A reduced performance compared to the plant based natural fibre materials is observed for the mineral fibre material, i.e., basalt fiber. This is attributed to the substitution of the UD plies in the spar caps in addition to the glass biaxial laminates in shells and webs. A similar substitution using plant based natural fibres would probably result in considerably heavier blade designs since strength properties are inferior compared to the ones of glass fibres. Therefore, direct comparison of basalt fibres against the other natural fibres and extraction of useful conclusions needs some careful thought. Regarding resins, thermoplastic one seems to give the most promising blade mass reduction up to 4.7%.

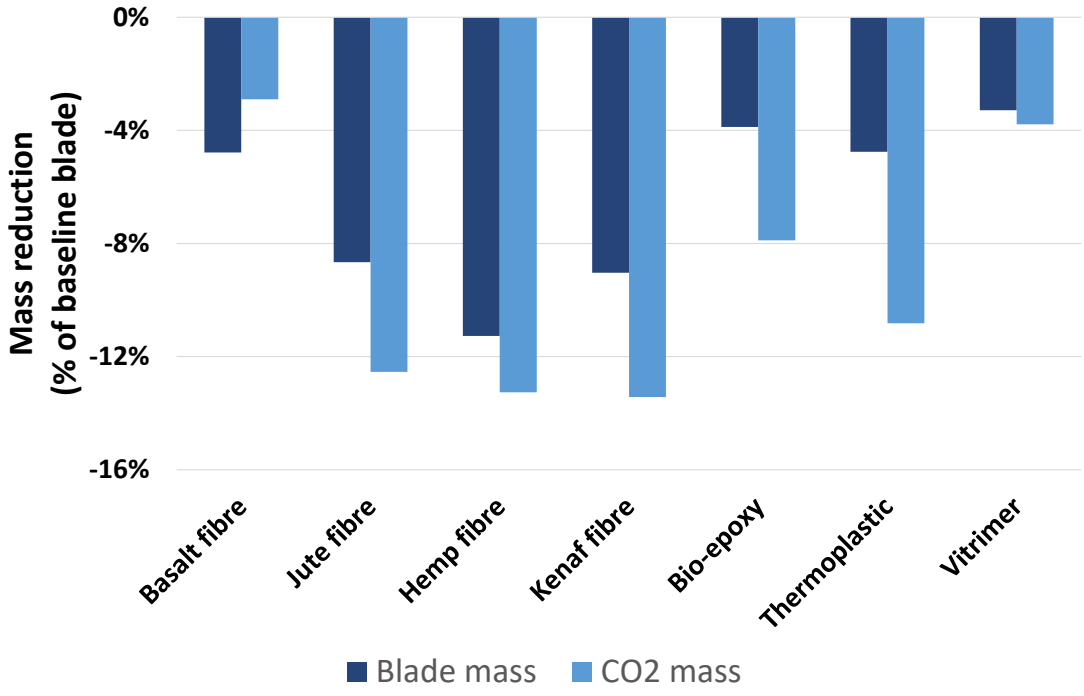

Figure 16 Blade and CO_2 mass change of the new blade designs.

It is highlighted that material properties used in this exercise were derived from micro mechanical models and thus, the actual reductions could be different from the ones displayed in

Figure 16, if experimental material property values were provided. Nevertheless, it is expected that if any change in these values, this should be minor because stiffness properties estimated from micro mechanical models correlate quite well with experimentally measured property values [15] and as discussed previously, design driver for the regions that materials were replaced is mainly stiffness. Furthermore, a source that could potentially affect the results in

Figure 16 is the initial design (starting point) of the optimization process as discussed in section 3.3.1. For all the alternative designs the starting point was the optimized baseline one. Nevertheless, gradient based optimization algorithms do not guarantee convergence to the global minimum point, and they do not provide any evidence whether the achieved convergence concerns a global or a local minimum one. This means that the designs with the global minimum modified LCoE value could potentially have not been identified yet and this would change accordingly the values of the associated blade masses. Making this even more complex, a starting point that could possibly result in global minimum modified LCoE value for a blade design would not necessarily give a global minimum for another blade design (with different materials) since changing materials affect the shape of the objective function and thus the same starting point could be trapped in a local minimum. Thus, attention on extracting any solid outcome from the results in

Figure 16 should be paid.

Regarding the equivalent CO_2 masses, again plant based natural fibres indicate the best performance with a reduction of up to 13.4% for Kenaf fibre and 13.2% for the industrial Hemp fibres. From

Figure 16, it seems that the blade design with the minimum CO_2 footprint (Kenaf design) is not necessarily at the same time the one with the minimum mass (Hemp design). However, uncertainty related to the identification of the global minimum could possibly alter this trend. Regarding resins, thermoplastic ones exhibit a good reduction of CO_2 of 10.8%. It is highlighted that the GWP values presented in Table 9 to Table 13 correspond to the fabrication of the virgin materials and they do not capture the whole life of each material in the product. Thus, results in

Figure 16 are limited to the effect of fabricating a virgin blade.

Overall, it can be said that appropriate regions have been identified to replace standard materials whilst industrial Hemp fibres provide the best solution with significant reductions both in blade and CO_2 mass. Nevertheless, considering that the identification of the global minima is not guaranteed by the optimization method implemented thus, the outcome of this work should be always treated carefully.

Several other factors should be considered before proceeding to the replacement of standard materials with natural fibre materials or alternative resins such as availability of these materials, capability to scale up their production, their cost and most important end of life strategies to assess the overall impact to the environment. Investigating costs for Hemp fibres as well as the yield capacity (per year) of a field with Hemp plant it was found that the going market for industrial Hemp fiber is about $260 per ton (£0.22 per kg), with the average yield being approximately 2.5 tons of Hemp fibre per acre [16]. Knowing that the Hemp fibre laminates in the respective blade design of

Figure 16 weight 15.8 ton and the Hemp fibre weight fraction is 58.3% then the Hemp fibre mass per blade is equal to 9.2 ton. Performing some simple calculations and conversions, the production of 9.2 ton of Hemp fibre would imply an area of approximately 0.0149 km^2 to be cultivated. Assuming that a typical annual production volume of wind turbine rotor blades is about 300 blades per year then the requirements for land would be about 4.5 km^2 to produce the necessary amount of Hemp fibres. To give an indication of the size of this area, the registered land (area) that was used to cultivate wheat in the UK in 2021 was about 17,900 km^2 [17] which is 3,981 times bigger than the needs for Hemp cultivation. Still however, land needs for Hemp cultivation cannot be neglected considering that this 4.5 km^2 mainly concerns the annual production volume of only one factory.

Regarding the overall impact to the environment, a lifecycle assessment from "cradle to gate" of the derived blade designs has been performed by NCC whilst it is documented in [18]. Main outcome is that it is necessary to select the appropriate end of life strategy for the blades. Comparing different landfilled and recycling approaches the study indicated that Vitrimer can give a reduction of the blade lifetime GWP value up to 18%. This is equivalent of up to 70-tonnes reduction in CO2 eq per blade. Furthermore, all materials enabled lower impact blades compared to the baseline one. However, plant-based fibres indicated the least reduction in the blade lifetime GWP value with a value less than 7%.

4 Conclusions

Various sustainable material systems were investigated and assessed for their capability to meet the performance requirements of a rotor blade. State of the art design tools were used to minimise blade CO_2 footprint whilst new promising designs were emerged. All the examined material systems provided lighter designs compared to the baseline blade design. Hemp fibres material system, however, seems to give the most promising blade and CO_2 mass reductions of up to 11.3% compared to the baseline one. Nevertheless, because of the use of gradient based optimisation methods, the outcome of this work should be always treated carefully. It was pointed out the role of the starting point in the optimization process. Furthermore, the study revealed that an area of 4.5 km^2 should be cultivated with industrial Hemp plant to cover the demands in Hemp fibres per year for a wind turbine blade factory. This is not a negligible amount of area and further feasibility studies should be contacted to prove the concept for the use of plant based natural fibres in the manufacturing of wind turbine blades.

The AM core has greater mass than a conventional core at low panel thickness because the larger mass of the face skins are not offset by the elimination of resin material being absorbed into the kerf cuts. A 5% additive infill density is unlikely to be able to withstand vacuum pressure, and a 10% infill density will reduce the competitiveness with conventional core materials as shown in the carpet plots in section 3.2.2. Beyond a 10% infill density there are no core materials in the standard reference blade which are thick enough to allow the AM core to beat a conventional core on infused weight, so a core with wall thickness of 1mm and an infill density of 7.5% will be used as a starting point for any future work.

For reusable silicone bags, a basic cost analysis was shown to give mixed results. The model was run for 30, 150 and 300 pulls. If the silicone bag were to survive 30 mould pulls, it shows a cost benefit – however it is important to note that with this lifetime the duration for which the mould would need to be out of action to spray up a new silicon vacuum bag would become significant (this has not been accounted for in the current costing). Likewise, after 30 mould pulls, the mass of waste vacuum bags would be greater than the mass of bagging film which it replaces. For 150 pulls the benefit is only marginal, at 300 pulls there is a clear benefit in terms of mass of material saved going to landfill. At 30 pulls, there is a cost saving of 0.4% compared with the baseline, at 150 pulls it is 1.3%, and at 300 pulls it is 1.4%. However, there would need to be a significant increase in blade manufacturing throughput to achieve a 300 blades per year target to achieve a balance between mass of wastage and cost savings. To justify the high up-front cost more work would be necessary to understand how many cycles the bags can last for as this is clearly extremely important for both the business case and the environmental case. However bag life is affected by numerous factors, storage conditions (e.g. temperature/humidity, handling), resin infusion chemistry, bag material and design, and number of pulls. Blade OEMs will likely need to be consulted to provide some of these inputs for any future endeavour into reusable bagging solutions.

Concluding, this work highlights the potential for more environmentally friendly blades to be produced without compromising performance of the blade whilst provides the industry with knowledge and tools to achieve their stated targets of net-zero emissions, fully recyclable and zero waste blades.

5 References

[1] W. C. AG.

[2] T. Macquart, V. Maes, D. Langston and A. Pirrera, “A New Optimisation Framework for Investigating Wind Turbine Blade Designs,” in *12th World Congress of Structural and Multidisciplinary Optimization, ISSMO*, Braunschweig, 2017.

[3] S. Scott, P. Greaves, P. M. Weaver, A. Pirrera and T. Macquart, “Efficient structural optimisation of a 20 MW wind,” in *Journal of Physics: Conference Series, The Science of Making Torque from Wind (TORQUE 2020)*, Delft, 2020.

[4] S. Scott, T. Macquart, C. Rodriguez, P. Greaves, P. McKeever, P. Weaver and A. Pirrera, “Preliminary validation of ATOM: an aero-servo-elastic design tool for next generation,” in *Conference Series: Journal of Physics, WindEurope*, Bilbao, 2019.

[5] K. Svanberg, “MMA and GCMMA - two methods for nonlinear optimization,” Optimization and Systems, 2007.

[6] *IEC 61400-1: Wind turbines -Part 1: Design requirements, 3rd IEC,* International Electrotechnical Commission, 2005.

[7] O. Nixon-Pearson, D. Mamalis and L. Stevenson, "WP4 INNOVATION IN LOW CARBON DESIGN AND MANUFACTURABILITY – Wind Turbine Blades Design and Manufacturing, current State-of-the Art Literature Review," ORE Catapult, 2021.

[8] *SR InfuGreen 810: Green Epoxy systems for Injection and Infusion,* Sicomin Epoxy Systems, 2017.

[9] *ELIUM180: Liquid Thermoplastic Resin,* ARKEMA.

[10] *VITRIMAX T130,* Mallinda Inc..

[11] *Basalt fibres,* LBIE: Lance Brown Import-Export.

[12] *Biotex Jute 2x2 Twill 550g/m2 Fabric,* easycomposites, 2013.

[13] A. Lotfi, H. Li, S. V. Dao and G. Prusty, "Natural fiber–reinforced composites: A review on material, manufacturing and machinability," *Journal of Thermoplastic Composite Materials,* pp. 1-47, 2019.

[14] A. Rashdi, S. M. Sapuan, M. Ahmad and K. Abdan, "Review of kenaf fiber reinforced polymer composites," *Polimery-Warsaw,* vol. LIV, pp. 775-888, 2009.

[15] E. J. Barbero, in *Introduction to composite materials design*, CRC Press, 2011.

[16] "bonafideseeds," Bonafide Seeds, 2022. [Online]. Available: https://www.bonafideseeds.com/how-much-can-i-make-hemp-farming-profit-per-acre/. [Accessed 26 10 2022].

[17] "Agriculture in the United Kingdom 2021," gov.uk, [Online]. Available: https://www.gov.uk/government/statistics/agriculture-in-the-united-kingdom-2021/chapter-7-crops. [Accessed 26 10 2022].

[18] P. Greaves, *Innovative design and lifecycle assessment of wind turbine blades using sustainable materials: A feasibility study-SUSWIND,* ORE Catapult, 2022.

CATAPULT
Offshore Renewable Energy

GLASGOW

ORE Catapult
Inovo
121 George Street
Glasgow
G1 1RD

+44 (0)333 004 1400

BLYTH

National Renewable
Energy Centre
Offshore House
Albert Street, Blyth
Northumberland
NE24 1LZ

+44 (0)1670 359555

LEVENMOUTH

Fife Renewables Innovation
Centre (FRIC)
Ajax Way
Leven
KY8 3RS

+44 (0)1670 357649

GRIMSBY

O&M Centre of Excellence
ORE Catapult, Port Office
Cleethorpe Road
Grimsby
DN31 3LL

+44 (0)333 004 1400

ABERDEEN

Subsea UK
30 Abercrombie Court
Prospect Road, Westhill
Aberdeenshire
AB32 6FE

07436 389067

CORNWALL

Hayle Marine Renewables
Business Park
North Quay
Hayle, Cornwall
TR27 4DD

+44 (0)1872 322 119

PEMBROKESHIRE

Marine Energy Engineering
Centre of Excellence (MEECE)
Bridge Innovation Centre
Pembrokeshire Science
& Technology Park
Pembroke Dock, Wales
SA72 6UN

+44 (0)333 004 1400

CHINA

11th Floor
Lan Se Zhi Gu No. 15
Ke Ji Avenue,
Hi-Tech Zone
Yantai City
Shandong Province
China

+44 (0)333 004 1400

LOWESTOFT

OrbisEnergy
Wilde Street
Lowestoft
Suffolk
NR32 1XH

01502 563368